AN ABSTRACT OF THE THESIS OF

CHUN-PANG CHIU for the MASTER OF SCIENCE
(Name) (Degree)

in Electrical and Electronics Engineering presented on Aug 12, 1969
(Major) (Date)

Title: ACTIVE NETWORK SYNTHESIS USING GYRATORS

Abstract approved: Redacted for Privacy
Leland C. Jensen

The paper is a study of (i) the realization of the gyrator, (ii) active filter synthesis using gyrator.

Several realization methods of the gyrator are summararized. A practical gyrator composed of two operational amplifiers was built and tested. The experimental results are shown. Two RC-gyrator synthesis techniques are derived and discussed. One method is to replace the inductors in a conventional LC filter with gyrators and capacitors. The other method is the application of Calahan's optimum polynomial decomposition to the synthesis procedure. The sensitivity of the two synthesis techniques are compared and discussed. A practical active filter was synthesized by the second method. The experimental results are shown.

Active Network Synthesis Using Gyrators

by

Chung-Pang Chiu

A THESIS

submitted to

Oregon State University

in partial fulfillment of
the requirements for the
degree of

Master of Science

June 1970

APPROVED:

Redacted for Privacy

Associate Professor of Electrical and Electronics Engineering

in charge of major

Redacted for Privacy

Head of Department of Electrical and Electronics Engineering

Redacted for Privacy

Dean of Graduate School

Date thesis is presented Aug 12, 1969

Typed by Clover Redfern for Chung-Pang Chiu

ACKNOWLEDGMENT

The author wishes to thank Professor Leland C. Jensen who suggested the topics of this thesis and gave much assistance, instruction and encouragement during the course of this study.

TABLE OF CONTENTS

LIST OF FIGURES

LIST OF TABLES

Table | | Page

ACTIVE NETWORK SYNTHESIS USING GYRATORS

I. INTRODUCTION

Over the past decade, increasing interest has been shown in synthesis techniques using active elements. Conventionally, the elements used in network synthesis are resistors, capacitors, inductors and transformers. Since capacitive elements are usually cheaper, simpler and more nearly ideal elements than are inductors, synthesis techniques using only RC elements are very important. On the other hand, non-positive real functions cannot be realized by using passive elements alone. The use of active devices will overcome some of these difficulties. The most commonly used active elements are negative resistances, controlled sources, operational amplifiers, negative impedance converters and gyrators. The gyrator is one of the most useful active elements. It has the property that it can gyrate an impedance into an admittance, and vice versa. By this property, an inductor can easily be obtained by terminating a gyrator with a capacitor. It is also attractive in microminiaturization, since the fabrication of inductors in thin-film and integrated-circuit technology is the most difficult problem, especially, for low frequency application, and no practical values of inductance have been obtained at this time.

The thesis will concentrate on gyrator synthesis techniques with sensitivity considerations. Sensitivity has been recognized as one of the main considerations in active RC synthesis. Chapter II gives some definitions of sensitivity. In Chapter III, optimum polynomial decompositions, developed by Horowitz and Calahan, are summarized. Butterworth and Chebyshev polynomials using this technique are decomposed and tabulated for practical use. The properties and realization methods of gyrator are described in Chapter IV. An actual circuit is synthesized and tested and the results also shown. Two RC-gyrator synthesis techniques are described and compared in Chapter V.

II. DEFINITION OF SENSITIVITY

Sensitivity is a measure of the degree of dependence of one quantity upon the value of another quantity. In network synthesis, the sensitivity is a measure of the change in certain network functions resulting from the change of the network elements. In this chapter, some definitions of sensitivity which have been used in network synthesis are defined.

1. Classical Sensitivity

Let $N(s, x_1, x_2, \ldots, x_n)$ be a network function of n parameters. For a single parameter case, $N(s, x)$, the sensitivity is defined as

$$S_x^N(s, x) = \frac{dN/N}{dx/x} = \frac{d \ln N}{d \ln x} = \frac{dN}{dx} \cdot \frac{x}{N}. \tag{2-1}$$

Since,

$$\ln N\,(j\omega, x) = \ln |N(j\omega, x)| + j \operatorname{Arg} N(j\omega, x). \tag{2-2}$$

equation (2-1) can be written as,

$$S_x^N(j\omega, x) = x\left(\frac{dM}{dx} + j\,\frac{d\theta}{dx}\right), \tag{2-3}$$

where

$$M = \ln |N(j\omega, x)|, \tag{2-4a}$$

$$\theta = \operatorname{Arg}[N(j\omega, x)]. \tag{2-4b}$$

Thus the real part of the sensitivity is the change in magnitude of the network functions, and the imaginary part of the sensitivity is the change in phase function.

Let $Q(s,x)$ and $P(s,x)$ be the numerator and the denominator of $N(s,x)$ respectively. Then

$$N(s,x) = \frac{Q(s,x)}{P(s,x)} . \tag{2-5}$$

It can be shown that

$$S_x^N(s,x) = x\left(\frac{Q'}{Q} - \frac{P'}{P}\right) , \tag{2-6}$$

where

$$Q' = \frac{\partial Q}{\partial x}, \quad P' = \frac{\partial P}{\partial x}. \tag{2-7}$$

2. Root Sensitivity

Let the network function $N(s,x) = \dfrac{Q(s,x)}{P(s,x)}$. The root sensitivity is defined as the change of the roots of $N(s,x)$ with respect to the change in one of the network parameters. Thus the root sensitivity can be expressed as

$$S_x^{s_j}(s,x) = \frac{ds_j}{dx/x} = x\,\frac{ds_j}{dx} . \tag{2-8}$$

If

$$P(s,x) = A(s) + xB(s), \tag{2-9}$$

then the pole sensitivity $S_x^{p_j}$ is

$$S_x^{p_j}(s, x) = x \frac{dp_j}{dx} = - \frac{xB(p_j)}{P'(p_j)} . \tag{2-10}$$

Similarly, let

$$Q(s, x) = C(s) + xD(s) \tag{2-11}$$

The zero sensitivity $S_x^{z_i}$ is

$$S_x^{z_i}(s, x) = x \frac{dz_i}{dx} = - \frac{xC(z_i)}{Q'(z_i)} . \tag{2-12}$$

3. Multiparameter Sensitivity

Let N be the network function with n parameters, $x_1, x_2, \ldots, x_n$.

$$N = N(s, x_1, x_2, x_3, \ldots, x_n). \tag{2-13}$$

Taking the partial derivatives with respect to each variable, x_n, the total differential is

$$dN = \frac{\partial N}{\partial x_1} dx_1 + \frac{\partial N}{\partial x_2} dx_2 + \ldots + \frac{\partial N}{\partial x_n} dx_n \tag{2-14}$$

Divide both sides by N

$$\frac{dN}{N} = d(\ln N) = \sum_i \frac{\partial \ln N}{\partial \ln x_i} (d \ln x_i). \tag{2-15}$$

The multiparameter sensitivity $\vec{S}^N$ may be defined as a gradient vector with elements $\frac{\partial \ln N}{\partial \ln x_i}$.

Let $d(\ln \vec{x}_i)$ be a vector with elements $d(\ln \vec{x}_i)$. Then

$$\frac{dN}{N} = (\vec{S}^N) d(\ln \vec{x}_i) \tag{2-16}$$

The multiparameter sensitivity $\vec{S}^N$ is then defined

$$\vec{S}^N = \text{Grad}\{(\ln N) \quad d(\ln \vec{x}_i)\} \tag{2-17}$$

4. The Relationship Between Classical Sensitivity and Root Sensitivity

Start from the definition of classical sensitivity,

$$S_x^N(s, x) = \frac{dN/N}{dx/x} = \frac{d(\ln N)}{d(\ln x)},$$

and define

$$N(s, x) = \frac{Q(s, x)}{P(s, x)} = \frac{C(s)+xD(s)}{A(s)+xB(s)}. \tag{2-18}$$

Then

$$S_x^N(s, x) = x\left(\frac{Q'}{Q} - \frac{P'}{P}\right) = x\left(\frac{D(s)}{Q(s, x)} - \frac{B(s)}{P(s, x)}\right). \tag{2-19}$$

Replace x by $x + \Delta x$. The poles of $N(s, x)$ will be determined by the root of equation

$$A(s) + (x+\Delta x)B(s) = 0. \tag{2-20}$$

Define

$$F(s, x) = \frac{xB(s)}{P(s, x)} . \tag{2-21}$$

Then Equation (2-20) can be written as

$$1 + \frac{\Delta x}{x} F(s, x) = 0 . \tag{2-22}$$

Assume the degree of the numerator of $F(s, x)$ is lower than the degree of the denominator. Then

$$F(s, x) = \sum_j \frac{k_j}{s - p_j} \tag{2-23}$$

Substitute (2-23) into (2-22), and examine the behavior of the equation in the vicinity of the jth pole of $F(s, x)$. Equation (2-22) may be written in the form

$$1 + \frac{\Delta x}{x} \frac{k_j}{p_j' - p_j} = 0 \tag{2-24}$$

where p_j' is the value of s which satisfies the equation. If we write $p_j' - p_j = \Delta p_j$, substitute it into Equation (2-24), rearrange and take the limit

$$\lim_{\Delta x \to 0} \frac{\Delta p_j}{\Delta x} = \frac{dp_j}{dx} = - \frac{1}{x} k_j . \tag{2-25}$$

Thus, the sensitivity of jth zero of $N(s, x)$ is

$$S_x^{p_j}(s, x) = \frac{dp_j}{dx/x} = -k_j, \tag{2-26}$$

Similarly, define

$$G(s, x) = \frac{xD(s)}{Q(s)} = \sum_i \frac{k_j}{s - z_i}, \tag{2-27}$$

The sensitivity of jth zero of $N(s, x)$ is

$$S_x^{z_i}(s, x) = \frac{dz_i}{dx/x} = - k_i , \tag{2-28}$$

Substitute (2-26) and (2-28) into (2-23) and (2-27) respectively. Thus

$$F(s, x) = \sum_j \frac{-S_x^{p_j}}{s - p_j}, \tag{2-29}$$

$$G(s, x) = \sum_i \frac{-S_x^{z_i}}{s - z_i}. \tag{2-30}$$

Substitute (2-29) and (2-30) into (2-19), the relation between classical sensitivity and root sensitivity results

$$S_x^N(s, x) = \sum_j \frac{S_x^{p_j}}{s - p_j} - \sum_i \frac{S_x^{z_i}}{s - z_i}. \tag{2-31}$$

III. POLYNOMIAL DECOMPOSITION IN ACTIVE NETWORK SYNTHESIS

In the previous chapter some sensitivity definitions have been stated. However, the synthesis technique based on the sensitivity consideration is very important and will be discussed here. Most of the active RC synthesis methods are based upon the partitioning of network functions into subnetwork functions. There are two decomposition forms.

1. RC-NIC Decomposition

Several methods have been presented to realize the immittance function by RC-NIC circuit. Horowitz (7) suggested a method by which a given polynomial can be decomposed into the difference of two other polynomials in such a way as to minimize the sensitivity. Calahan (4) has also shown that the same method can minimize the root sensitivity.

Let

$$
\begin{aligned}
P(s,k) &= a_n s^n + a_{n-1} s^{n-1} + \dots + a_0 \\
&= A_{on} A_n(s) - kB_{on} B_n(s) \\
&= \sum_{i=0}^{n} (a_i - kb_i) s^i = \sum_{i=0}^{n} a_i s^i
\end{aligned}
\qquad (3\text{-}1)
$$

where

$$A_n(s) = \prod_{1}^{n/2} (s+a_i), \tag{3-2a}$$

$$B_n(s) = \prod_{1}^{n/2} (s+b_i) \tag{3-2b}$$

$$\alpha_i = a_i - kb_i \tag{3-2c}$$

The sensitivity of any change of coefficient α_i with respect to k is

$$S_k^{\alpha_i} = \frac{\partial \alpha_i}{\partial k} \frac{k}{\alpha_i} = - \frac{kb_i}{\alpha_i} \ . \tag{3-3}$$

In order to minimize the sensitivity to the change of any coefficient in k, it is necessary to minimize the corresponding coefficient of $B_{on}B_n(s)$. Horowitz (7) has shown that the polynomial $P(s)$ must be decomposed into two new polynomials; $a^2(s)$ and $sb^2(s)$. These polynomials have zeros arranged as shown in Figure 3-1.

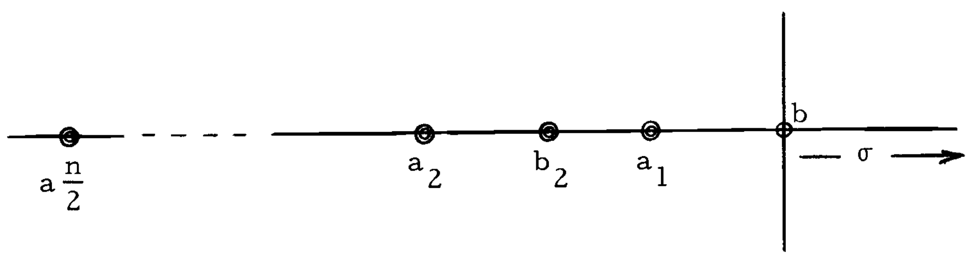

Figure 3-1. Optimum zero pattern of RC-NIC decomposition.

The optimum pattern can thus be written as

$$P(s) = \alpha_n s^n + \alpha_{n-1} s^{n-1} + \dots + \alpha_0$$

$$= a^2(s) - B_o s b^2(s), \qquad (3\text{-}4)$$

where

$$a(s) = (s+a_1)(s+a_2) \dots (s+a_{n/2}) \qquad (3\text{-}5a)$$

$$b(s) = (s+b_2)(s+b_3) \dots (s+b_{n/2-1}) \qquad (3\text{-}5b)$$

The optimum decomposition of the polynomial $P(s)$ can be obtained by the following procedures:

1) Form the polynomial $P(s^2)$: that is the polynomial formed by replacing s with s^2. Let $F(s)$ contain the left half-plane roots of $P(s^2)$. Obviously, $F(s)$ is Hurwitz and $F(-s)$ contains the right half plane roots of $P(s^2)$. Thus we obtain

$$P(s^2) = F(s)F(-s). \qquad (3\text{-}6)$$

2) Since $F(s)$ is Hurwitz, $F(s)$ can be expressed as

$$F(s) = A(s) + sB(s), \qquad (3\text{-}7)$$

then

$$P(s^2) = A^2(s) - s^2B^2(s). \qquad (3\text{-}8)$$

3) Replace s with s^2 in the optimum form of Equation (3-4) which yields

$$P(s^2) = a^2(s^2) - B_o s^2 b^2(s^2). \qquad (3\text{-}9)$$

Compare Equation (3-8) and (3-9),

$$A(s) = a(s^2), \qquad (3\text{-}10a)$$

$$B(s) = \sqrt{B_o}\, b(s^2). \qquad (3\text{-}10b)$$

4) Substitute (3-10a) and (3-10b) into (3-8) and replace s with s^2, the optimum form results

$$P(s) = a^2(s) - B_o s b^2(s). \qquad (3\text{-}11)$$

(Example):

Find the RC-NIC optimum decomposition of

$$P(s) = s^2 + \beta_1 s^2 + \gamma_1. \qquad (3\text{-}12)$$

Apply the procedures

1) $P(s^2) = s^4 + \beta_1 s^2 + \gamma_1$

$$= [(s^2+\sqrt{\gamma_1}) + s\sqrt{2\sqrt{\gamma_1}-\beta_1})] \cdot [(s^2+\sqrt{\gamma_1}) - s\sqrt{2\sqrt{\gamma_1}-\beta_1}].$$

2) $F(s) = (s^2+\sqrt{\gamma_1}) + s \cdot (\sqrt{2\sqrt{\gamma_1}-\beta_1}).$

3) $a(s^2) = s^2 + \sqrt{\gamma_1}$, and

$B_o b(s^2) = \sqrt{2\sqrt{\gamma_1} - \beta_1}$.

4) Finally the optimum form results

$$P(s) = (s+\sqrt{\gamma_1})^2 - s(2\sqrt{\gamma_1} - \beta_1). \tag{3-13}$$

2. RC-RL Decomposition

Since and equivalent inductor can be obtained by terminating a gyrator with a capacitor, RC-RL decomposition can also be applied in RC-gyrator synthesis.

Let

$$\begin{aligned} P(s) &= a_n s^n + a_{n-1} s^{n-1} + \ldots + a_0 \\ &= \prod_1^{n/2} (s+s_i)(s+\bar{s}_i) \\ &= A_{on} A_n(s) + kB_{on} B_n(s), \end{aligned} \tag{3-14}$$

where

$$A_n(s) = \prod_1^{n/2} (s+a_i) \tag{3-15a}$$

$$B_n(s) = \prod_1^{n/2} (s+b_i) \tag{3-15b}$$

The zeros are distributed as in Figure 3-2.

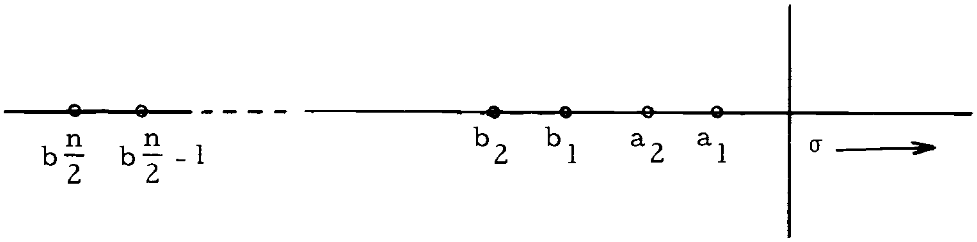

Figure 3-2. Zero pattern of $A_n(s)$ and $B_n(s)$.

The root sensitivity of Equation (3-14) is

$$|S_k^{s_i}| = \left|\frac{ds_i}{dk/k}\right| = \left|\frac{kB_{on}B_n(s_i)}{dP(s_i)/ds}\right| = \left|\frac{A_{on}A_n(s_i)}{P'(s_i)}\right|. \qquad (3\text{-}16)$$

The sensitivity will be minimized if $A_{on}A_n(s_i)$ is minimized. The optimum zeros pattern is shown in Figure 3-3.

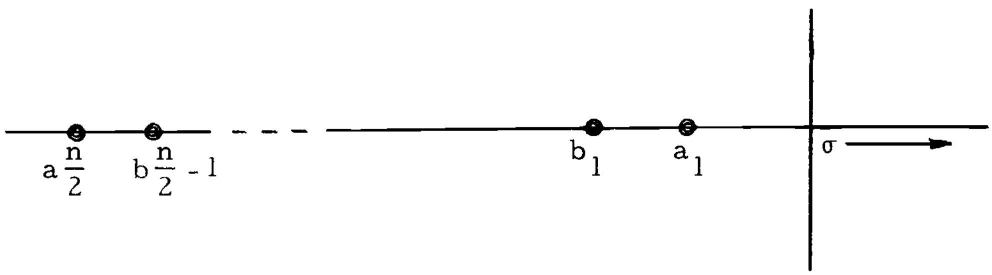

Figure 3-3. Optimum zero pattern of RC-RL decomposition.

Calahan (6) shows that if,

1) $$\sum_{i=1}^{n/2} \text{Arg } S_i \leq \frac{\pi}{2}, \qquad (3\text{-}17a)$$

A unique decomposition of $P(s)$ is possible and has the form

$$P(s) = \prod_{1}^{n/2} (s+a_i)^2 + B_{on} \prod_{1}^{(n/2)-1} (s+b_i)^2. \qquad (3\text{-}17b)$$

2) $$\sum_{i=1}^{n/2} \operatorname{Arg} S_i < \frac{\pi}{2}, \qquad (3\text{-}18a)$$

Non-unique decompositions of $P(s)$ are possible and have the form

$$P(s) = A_{on} \prod_{1}^{n/2} (s+a_i)^2 + B_{on} \prod_{1}^{n/2} (s+b_i)^2. \qquad (3\text{-}18b)$$

For the unique decomposition case, let

$$A_{on} \prod_{1}^{n/2} (s+a_i)^2 = [R_m(s)]^2 \qquad (3\text{-}19a)$$

and

$$B_{on} \prod_{1}^{n/2} (s+b_i)^2 = [Q_m(s)]^2. \qquad (3\text{-}19b)$$

Then

$$R_m(s) = \sqrt{A}_{on} \prod_{1}^{n/2} (s+a_i), \qquad (3\text{-}20a)$$

$$Q_m(s) = \sqrt{B}_{on} \prod_{1}^{n/2} (s+b_i), \qquad (3\text{-}20b)$$

and

$$P(s) = \prod_{1}^{n/2} (s+s_i)(s+\bar{s}_i)$$

$$= [R_m(s)]^2 + [Q_m(s)]^2$$

$$= [R_m(s)+jQ_m(s)][R_m(s)-jQ_m(s)]. \tag{3-21}$$

Summarizing the above equations a procedure for finding optimum RC-RL decompositions obtained:

1) From a given polynomial

$$P(s) = \prod_{1}^{n/2} (s+s_i)(s+\bar{s}_i)$$

determine $R_m(s)$ and $Q_m(s)$.

2) Assign

$$[R_m(s)]^2 = A_{on} \prod_{1}^{n/2} (s+a_i)^2, \tag{3-22a}$$

$$[Q_m(s)]^2 = B_{on} \prod_{1}^{(n/2)-1} (s+b_i)^2. \tag{3-22b}$$

3) Substitute Equation (3-22a) and (3-22b) into (3-21) to get optimum RC-RL form.

For non-unique decomposition, equating the given polynomial to the optimum form and comparing the corresponding coefficients, it is found that there are $n+2$ unknowns and only $n+1$ equations.

Arbitrarily select the value of A_{on}/B_{on}. Infinite numbers of other decompositions can then be found. Calahan (6) also concludes that, for a given polynomial

$$P(s) = a_n s^n + a_{n-1} s^{n-1} + \ldots + a_0$$

$$= \prod_{1}^{n/2} (s+s_i)(s+\bar{s}_i)$$

$$= A_{on} A_n(s) + kB_{on} B_n(s). \tag{3-23}$$

If

$$\sum_{1}^{n/2} \text{Arg } S_i > \frac{\pi}{2}, \tag{3-24a}$$

only RC-NIC decomposition is possible. If

$$\sum_{1}^{n/2} \text{Arg } S_i \leq \frac{\pi}{2}, \tag{3-24b}$$

both RC-NIC and RC-RL decomposition are possible. The latter can always be chosen to have the lower sensitivity.

(Examples):

1) For a given polynomial

$$P(s) = s^2 + \beta_1 s + \gamma_1,$$

if

$$\text{Arg } S_1 = \text{Arg } \frac{\sqrt{4\gamma_1 - \beta_1^2}}{\beta_1} > \frac{\pi}{2} .$$

The optimum RC-NIC form can be found in the example on page 12. If

$$\text{Arg } S_1 = \text{Arg } \frac{\sqrt{4\gamma_1 - \beta_1^2}}{\beta_1} \leqq \frac{\pi}{2} ,$$

Apply the RC-RL decomposition procedure:

i) $$P(s) = (s+\frac{\beta_1}{2} + j\sqrt{\gamma_1 - \frac{\beta_1^2}{4}})(s+\frac{\beta_1}{2} - j\sqrt{\gamma_1 - \frac{\beta_1^2}{4}})$$

$$= [R_m(s)+jQ_m(s)][R_m(s)-jQ_m(s)].$$

ii) $$[R_m(s)]^2 = (s+\frac{\beta_1}{2})^2 .$$

$$[Q_m(s)]^2 = \gamma_1 - \frac{\beta_1^2}{4}.$$

iii) Thus the optimum RC-RL decomposition is

$$P(s) = (s+\frac{\beta_1}{2})^2 + (\gamma_1 - \frac{\beta_1^2}{4}) . \tag{3-25}$$

2) When $P(s) = (s^2+as+b)(s^2+cs+d)$ (3-26)

apply the angle criterion,

(Case 1):

$$\sum_{i=1}^{2} \operatorname{Arg} S_i = \operatorname{Arg} S_1 + \operatorname{Arg} S_2 = \operatorname{Arg} \frac{\sqrt{4b-a^2}}{a}$$

$$+ \operatorname{Arg} \frac{\sqrt{4d-c^2}}{c} > \frac{\pi}{2}. \quad (3\text{-}27)$$

Only RC-NIC decomposition is possible, the optimum form is

$$P(s) = a^2(s) - sb^2(s)$$

$$= [s^2+(\sqrt{b}+\sqrt{d}+\sqrt{(4\sqrt{bd}+ac)-2(c\sqrt{b}+a\sqrt{d})}+\sqrt{bd}]^2$$

$$- s[s(\sqrt{2\sqrt{b}-a}+\sqrt{2\sqrt{d}-c})+(\sqrt{2\sqrt{b}-a})d+\sqrt{(2\sqrt{d}-c)b})^2$$

$$(2\text{-}38)$$

(Case 2):

$$\operatorname{Arg} S_i = \operatorname{Arg} S_1 + \operatorname{Arg} S_2 = \operatorname{Arg} \frac{\sqrt{4b-a^2}}{a}$$

$$+ \operatorname{Arg} \frac{\sqrt{4d-c^2}}{c} \leqq \frac{\pi}{2}, \quad (3\text{-}29)$$

RC-RL decomposition has lower sensitivity than RC-NIC case. The RC-RL optimum form is

$$P(s) = [s^2+\frac{1}{2}(a+c)s+\frac{\sqrt{ac-(4b-a^2)(4d-c^2)}}{4}]^2$$

$$+ \frac{1}{2}[(\sqrt{4b-a^2}+\sqrt{4d-c^2})s+\frac{1}{2}(a\sqrt{4d-c^2}+c\sqrt{4b-a^2})]^2.$$

$$(3\text{-}30)$$

For practical design convenience, the decomposition of Butterworth and Chebyshev polynomials with degree from 2 to 5 have been constructed and tabulated (Tables 1-5). These are calculated by hand; for high degree cases the use of a digital computer is needed.

Table 1. Optimum RC-NIC and RC-RL decomposition forms of Butterworth polynomaisl.

n	$P(s) = P_1(s) \cdot P_2(s)$	$P_1(s)$	Optimum RC-NIC decompositions of $P_2(s)$	Optimum RC-RL decompositions of $P_2(s)$	Σ Arg S_i
2	$s^2 + 1.414s + 1$	1	$(s+1)^2 - 0.5858 \cdot s$	$(s+0.7071)^2 + 0.5$	$\frac{\pi}{4}$
3	$(s+1)(s^2+s+1)$	$s + 1$	$(s+1)^2 - s$	$(s+0.5)^2 + 0.75$	$\frac{\pi}{3}$
4	$(s^2+0.7854s+1) \times (s^2+1.8478s+1)$	1	$[(s+0.5250)(s+1.9050)]^2 - 2.5167s \cdot (s+1)^2$	$[(s+1.2247)(s+0.0919)]^2 + 3.3917(s+0.8446)^2$	$\frac{\pi}{2}$
5	$(s+1)(s^2+0.6180s+1) \times (s^2+1.6180s+1)$	$s + 1$	$[(s+2.2899s)(s+0.4367)]^2 -3.2205s \cdot (s+1)^2$		$107.91^{\circ} > \frac{\pi}{2}$

Table 2. Optimum RC-NIC and RC-RL decomposition forms of Chebyshev polynomials (with 1/2 db ripple).

n	$P(s) = P_1(s) \cdot P_2(s)$	$P_1(s)$	Optimum RC-NIC decompositions of $P_2(s)$	Optimum RC-RL decompositions of $P_2(s)$	Σ Arg S_i
2	$s^2 + 1.4256s + 1.5162$	1	$(s+1.2313)^2 - 1.0370s$	$(s+0.7128)^2 + 1.0081$	$54.62^\circ < \frac{\pi}{2}$
3	$(s+0.6264)$ $\times (s^2+0.6264s+1.1424)$	$s + 0.6264$	$(s+1.0688)^2 - 1.5112s$	$(s+0.3132)^2 + 1.0443$	$72.96^\circ < \frac{\pi}{2}$
4	$(s^2+0.3508s+1.0637)$ $\times (s^2+0.8466s+0.3564)$	1	$[(s+2.1095)(s+0.2922)]^2$ $- 3.6058 \cdot s \cdot (s+0.7328)^2$		$125.22^\circ > \frac{\pi}{2}$
5	$(s+0.3623)$ $\times (s^2+0.2240s+1.0359)$ $\times (s^2+0.5862s+0.4768)$	$s + 0.3623$	$[(s+0.2661)(s+2.6421)]^2$ $- 5.006(s+0.8208)^2$		$144.78^\circ > \frac{\pi}{2}$

Table 3. Optimum RC-NIC and RC-RL decomposition forms of Chebychev polynomial (with 1 db ripple).

n	$P(s) = P_1(s) \cdot P_2(s)$	$P_1(s)$	Optimum RC-NIC decompositions of $P_2(s)$	Optimum RC-RL decompositions of $P_2(s)$	Σ Arg S_i
2	$s^2 + 1.097s + 1.1025$	1	$(s+1.050)^2 - 1.0022s$	$(s+0.5489)^2 + 0.8012$	$58.49^\circ < \frac{\pi}{2}$
3	$(s+0.4942)$ $\times (s^2+0.4942s+0.9942)$	$s + 0.4942$	$(s+0.9971)^2 - 1.5000s$	$(s+0.2471)^2 + 0.9331$	$75.65^\circ < \frac{\pi}{2}$
4	$(s^2+0.2790s+0.9865)$ $\times (s^2+0.6736s+0.2794)$	1	$(s+2.0782)^2(s+0.2526)^2$ $- 3.7153(s+0.6977)^2$		$132.37^\circ > \frac{\pi}{2}$
5	$(s+0.2895)$ $\times (s^2+0.1790s+0.9882)$ $\times (s^2+0.4684s+0.4293)$	$s + 0.2895$	$(s+0.2475)^2(s+2.6365)^2$ $- 5.1203(s+0.7927)^2$		$154.44^\circ > \frac{\pi}{2}$

Table 4. Optimum RC-NIC and RC-RL decomposition forms of Chebychev polynomial (with 2 db ripple).

n	$P(s) = P_1(s) \cdot P_2(s)$	$P_1(s)$	Optimum RC-NIC decompositions of $P_2(s)$	Optimum RC-RL decompositions of $P_2(s)$	Σ Arg S_i
2	$s^2 + 0.8038s + 0.6366$	1	$(s+0.7979)^2 - 0.7920s$	$(s+0.4019)^2 + 0.4751$	$59.76^\circ < \frac{\pi}{2}$
3	$(s+0.3689)$ $\times (s^2+0.3688s+0.8861)$	$(s+0.3689)$	$(s+0.9413)^2 - 1.5138 \cdot s$	$(s+0.1844)^2 + 0.8521$	$78.69^\circ < \frac{\pi}{2}$
4	$(s^2+0.2098s+0.9285)$ $\times (s^2+0.5064s+0.2195)$	1	$(s+1.9620)^2(s+0.2301)^2$ $- 3.8191 \cdot s(s+0.6002)^2$		$141.20^\circ > \frac{\pi}{2}$
5	$(s+0.2183)$ $\times (s^2+0.1348s+0.9522)$ $\times (s^2+0.3532s+0.3931)$	$s + 0.2183$	$(s+0.2295)^2(s+2.6522)^2$ $- 5.2753 \cdot s(s+0.766)^2$		$160.04^\circ > \frac{\pi}{2}$

Table 5. Optimum RC-NIC and RC-RL decomposition forms of Chebychev polynomial (with 3 db ripple).

n	$P(s) = P_1(s) \cdot P_2(s)$	$P_1(s)$	Optimum RC-NIC decompositions of $P_2(s)$	Optimum RC-RL decompositions of $P_2(s)$	Σ Arg S_i
2	$s^2 + 0.6450s + 0.7080$	1	$(s+0.8414)^2 - 1.0378 \cdot s$	$(s+0.3225)^2 + 0.6040$	$67.47^\circ < \frac{\pi}{2}$
3	$(s+0.2986)$ $\times (s^2+0.2986s+0.8397)$	$s + 0.2896$	$(s+0.9163)^2 - 1.5340 \cdot s$	$(s+0.1493)^2 + 0.8174$	$80.63^\circ < \frac{\pi}{2}$
4	$(s^2+0.1704 \cdot s+0.9031)$ $\times (s^2+0.4112s+0.1959)$	1	$(s+0.2005)^2(s+2.0974)^2$ $- 3.9279 \cdot s \cdot (s+0.6135)^2$		$148.98^\circ > \frac{\pi}{2}$
5	$(s+0.1775)$ $\times (s^2+0.1096s+0.9329)$ $\times (s^2+0.2872s+0.3770)$	$(s+0.1775)$	$(s+0.0506)^2(s+1.8385)^2$ $- 5.3815 \cdot s \cdot (s+0.7611)^2$		$163.22^\circ > \frac{\pi}{2}$

IV. THE PROPERTIES AND REALIZATIONS OF GYRATOR

The gyrator, first investigated by B. D. Tellegen (15) in 1948, is a two port device in which the impedance seen at either port is the reciprocal of the impedance connected to the other port. By this property a current is gyrated into a voltage, an impedance into an admittance, and vice versa. In network synthesis, there are many advantages such as size and weight reduction to be realized from the elimination of inductors. Since the fabrication of the inductors in integrated circuits is not feasible, the gyrator will play an important role in the integrated inductor simulation.

1. The Origin of Gyrator

In order to create useful systems, besides the four known network elements--resistor, inductor, capacitor and transformer, we shall consider another similar element. By careful study, we find n-ports network composed of these elements have the properties of:

A) the relationships between the voltages and currents of the terminals is formed by a system of ordinary differential equations, with

B) constant coefficients;

C) the n-port is passive: it can deliver no energy, and

D) reciprocity holds.

Dropping any one of the first three properties will cause the system to become complicated. An n-port network possessing the first three properties but lacking the fourth may be very similar to the n-port network composed of four elements. We shall find a new type of network to realize these n-ports in which the first three properties hold but which violates the reciprocity theorem. This requirement has no significance for a one port element, such as C, R, and L, so we have to look for a new two port element. The ideal transformer is a type for which $i_1 v_1 + i_2 v_2 = 0$, as in the ideal case, energy can neither be dissipated nor stored. The equations for the ideal transformer are

$$i_1 = -ni_2, \tag{4-1a}$$

$$v_2 = nv_1, \tag{4-1b}$$

which satisfies the reciprocity relation. Another two-port element which satisfies $i_1 v_1 + i_2 v_2 = 0$, but violates reciprocity is described by

$$v_1 = -Ri_2, \tag{4-2a}$$

$$v_2 = Ri_1, \tag{4-2b}$$

and is named "ideal gyrator."

2. The Properties of the Gyrator

As stated previously, an ideal gyrator is a two port device whose terminal characteristics are described by

$$v_1 = -Ri_2, \tag{4-2a}$$

$$v_2 = Ri_1. \tag{4-2b}$$

The circuit symbol as shown in Figure 4-1 where "R" is called the "gyration resistance."

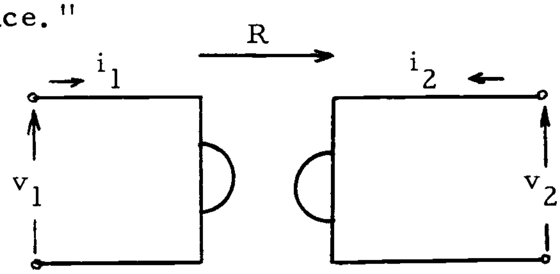

Figure 4-1. The circuit symbol of an ideal gyrator.

From Equation (4-2), the ideal gyrator can be described as the following matrices,

$$\text{Impedance matrix} \quad [Z] = \begin{bmatrix} 0 & R \\ R & 0 \end{bmatrix}, \tag{4-4}$$

$$\text{Admittance matrix} \quad [Y] = \begin{bmatrix} 0 & \frac{1}{R} \\ -\frac{1}{R} & 0 \end{bmatrix}, \tag{4-5}$$

$$\text{Transmission matrix} \; [T] = \begin{bmatrix} 0 & R \\ \frac{1}{R} & 0 \end{bmatrix}. \tag{4-6}$$

The following properties are derived from Equation (4-2).

A) An ideal gyrator is a passive and lossless device.

B) By connecting an impedance Z at the output terminal, an impedance $Z' = \frac{R^2}{Z}$ at the input terminal can be found.

This can be proven as follows: Figure 4-2 is an ideal gyrator with an impedance Z at the output terminals. Its matrix can be expressed as

$$\begin{bmatrix} 0 & R \\ \frac{1}{R} & 0 \end{bmatrix} \begin{bmatrix} 1 & Z \\ 0 & 1 \end{bmatrix} = \begin{bmatrix} 0 & R \\ \frac{1}{R} & \frac{Z}{R} \end{bmatrix} . \tag{4-7}$$

Figure 4-3 is an ideal gyrator with an impedance Z' between the input terminal. Its transmission matrix is:

$$\begin{bmatrix} 1 & 0 \\ \frac{1}{Z'} & 1 \end{bmatrix} \begin{bmatrix} 0 & R \\ \frac{1}{R} & 0 \end{bmatrix} = \begin{bmatrix} 0 & R \\ \frac{1}{R} & \frac{R}{Z'} \end{bmatrix} . \tag{4-8}$$

Comparing these two matrices, if $Z' = \frac{R^2}{Z}$, the two networks are equivalent.

C) An ideal transformer with unity turns ratio can be realized by two identical ideal gyrators in cascade. That is

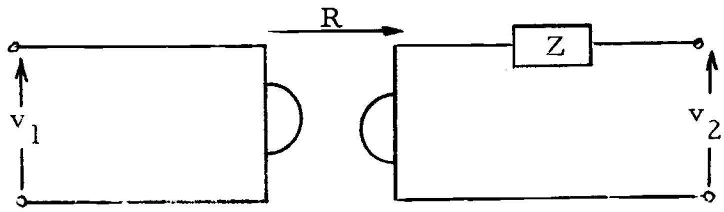

Figure 4-2. An ideal gyrator with an impedance Z at the output terminal.

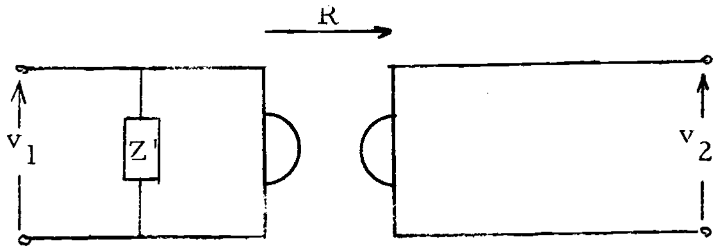

Figure 4-3. An ideal gyrator with an impedance Z' at the input terminal.

$$\begin{bmatrix} 0 & R \\ \frac{1}{R} & 0 \end{bmatrix} \begin{bmatrix} 0 & R \\ \frac{1}{R} & 0 \end{bmatrix} = \begin{bmatrix} 1 & 0 \\ 0 & 1 \end{bmatrix} \tag{4-9}$$

Schematically, the realization at an ideal transformer is shown in Figure 4-4.

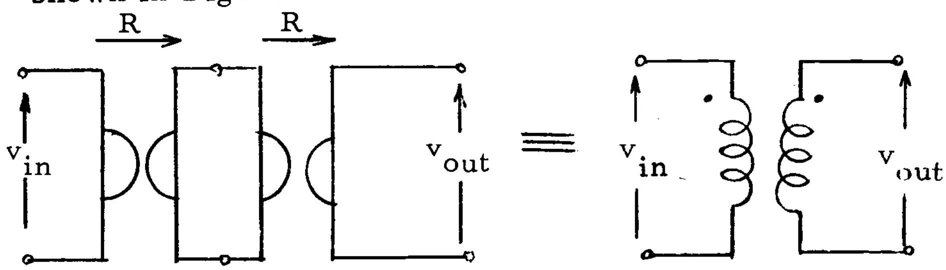

Figure 4-4. A realization of an ideal transformer.

D) A grounded inductor can be realized by an ideal gyrator terminated with a capacitor as shown in Figure 4-5.

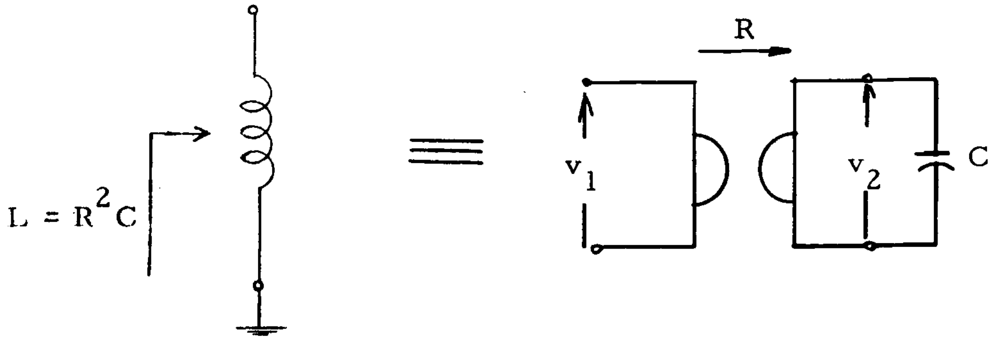

Figure 4-5. A realization of a grounded inductor.

E) An ungrounded inductor can be obtained by two gyrators and a capacitor as shown in Figure 4-6.

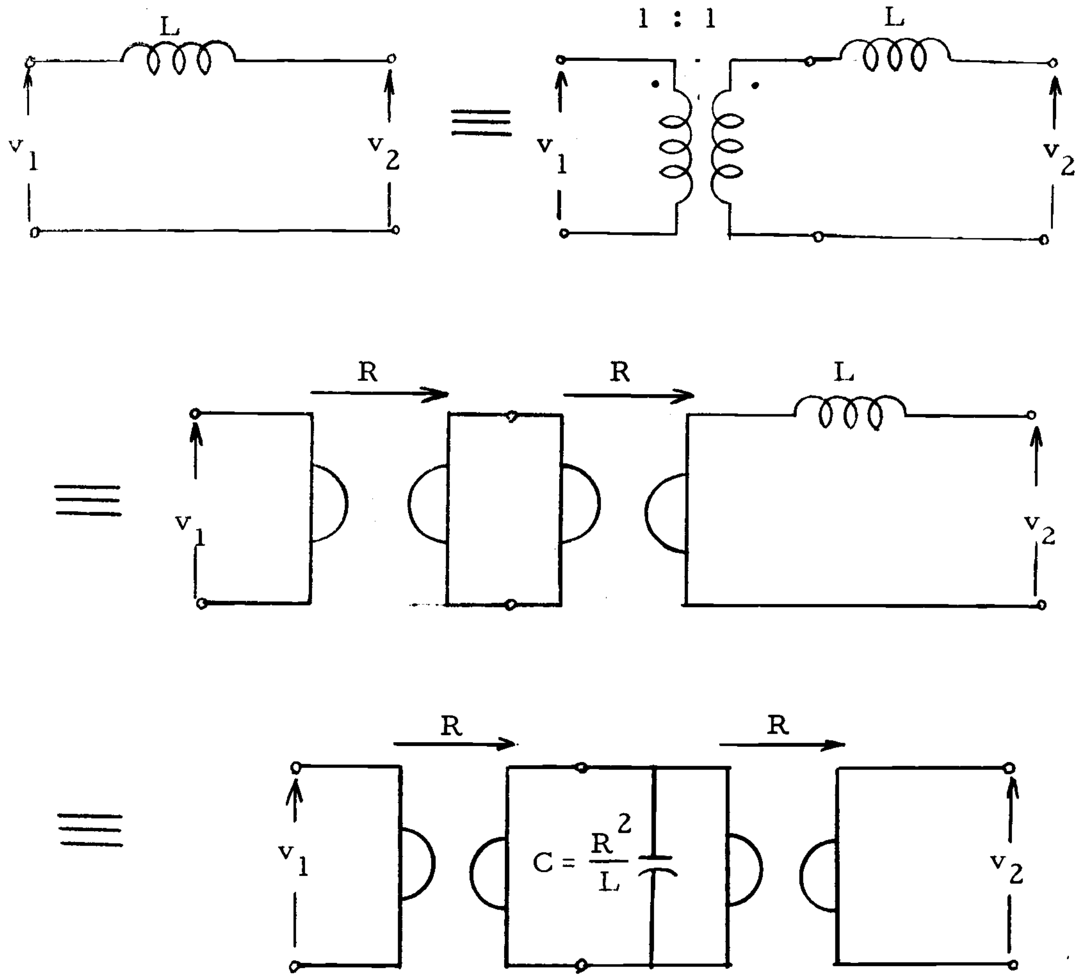

Figure 4-6. A realization of an ungrounded inductor.

3. The Realization of Gyrators

Since gyrators hold so many useful properties, it is very interesting to investigate its actual circuit realization. Briefly, the realization methods can be divided into three groups:

A) Realization by inseration of negative impedance elements to compensate for the residual positive input and output impedances.

B) Realization by two parallel VCCSs (voltage controlled current sources).

C) Realization by cascade NIC (negative impedance converter) and NIV (negative impedance inverter).

3a. Realization Using Negative Impedance Elements

Consider the feedback circuit of Figure 4-7. This circuit consists of an amplifier with input impedance Z_1, output impedance Z_2, and open circuit gain k.

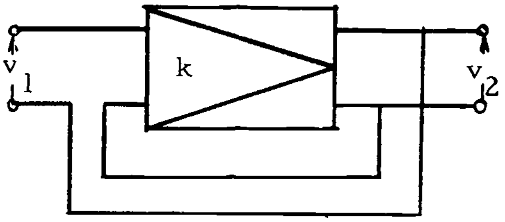

(a) Series-parallel connection

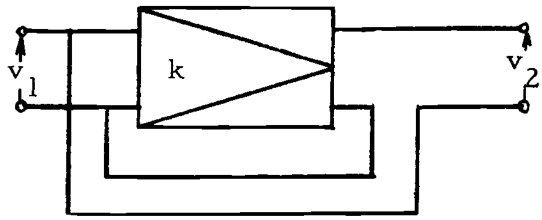

(b) Parallel-series connection

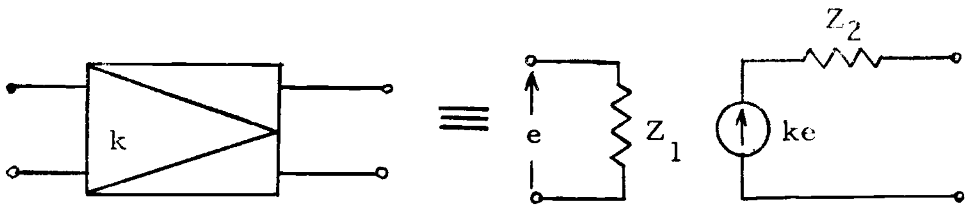

(c) Equivalent circuit of the amplifier

Figure 4-7. The feedback circuit connection.

For the series-parallel (s-p) and parallel-series (p-s) connections, we have the following impedance and admittance matrices:

Series-parallel:

$$[Z]_{s-p} = \begin{bmatrix} a & -Z_2 \\ Z_1 - a & Z_2 \end{bmatrix}, \tag{4-10}$$

Parallel-series:

$$[Z]_{p-s} = \begin{bmatrix} Z_1 & -Z_1 \\ Z_2 - a & a \end{bmatrix}, \tag{4-11}$$

Series-parallel:

$$[Y]_{s-p} = \begin{bmatrix} Y_1 & Y_1 \\ \alpha' - Y_2 & \alpha \end{bmatrix}, \tag{4-12}$$

Parallel-series:

$$[Y]_{p-s} = \begin{bmatrix} \alpha' & Y_2 \\ \alpha' - Y_1 & Y_2 \end{bmatrix}, \tag{4-13}$$

where

$$\begin{aligned} \alpha &= Z_1(1-k) + Z_2, \\ \alpha' &= Y_2(1-k) + Y_1, \\ Y_1 &= \frac{1}{Z_2}, \quad \text{and} \quad Y_2 = \frac{1}{Z_1}. \end{aligned} \tag{4-14}$$

If the output is terminated by impedance Z_L, then the input impedance of the series-parallel and parallel-series connections are:

Series-parallel

$$Z_{in} = \frac{Z_1 Z_2}{Z_2 + Z_L}, \tag{4-15}$$

Parallel-series

$$Z_{in} = \frac{Z_1(Z_2 + Z_L)}{Z_2}. \tag{4-16}$$

By inspection of Equation (4-10), (4-12) and (4-15), if the following conditions are satisfied, then a gyrator can be formed.

i) If $\alpha = 0$, then $K = 2$ and $Z_1 = Z_2 = R$, and

ii) if $Z_L \gg Z_2$, and

iii) if a series circuit is connected to a negative impedance (equal to Z_2) at the output or a parallel circuit is connected to a negative admittance (equal to Y_1) at the input.

Similarly, by inspection of Equations (4-11), (4-13) and (4-16), if the following conditions are satisfied, then a gyrator can be formed.

i) $\alpha = 0$, then $K = 2$ and $Z_1 = Z_2 = R$

ii) $Z_L \ll Z_2$

iii) a series circuit is connected to a negative impedance (equal to Z_1) at the input, or a parallel circuit is connected to a negative admittance (equal to Y_2) at the output.

The equivalent circuits are shown in the following figures.

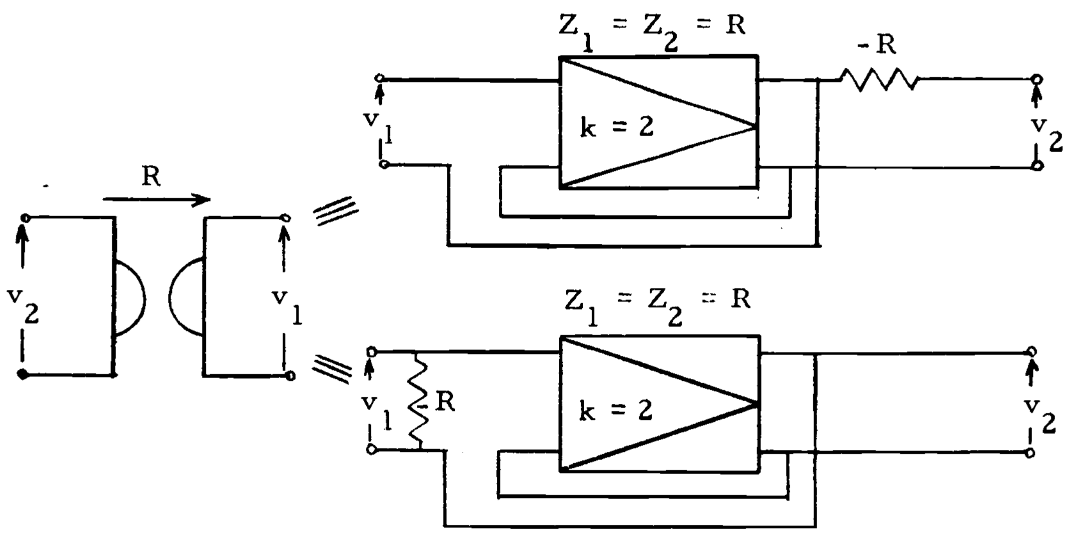

Figure 4-8. A realization of an ideal gyrator by s-p connection of the feedback circuit.

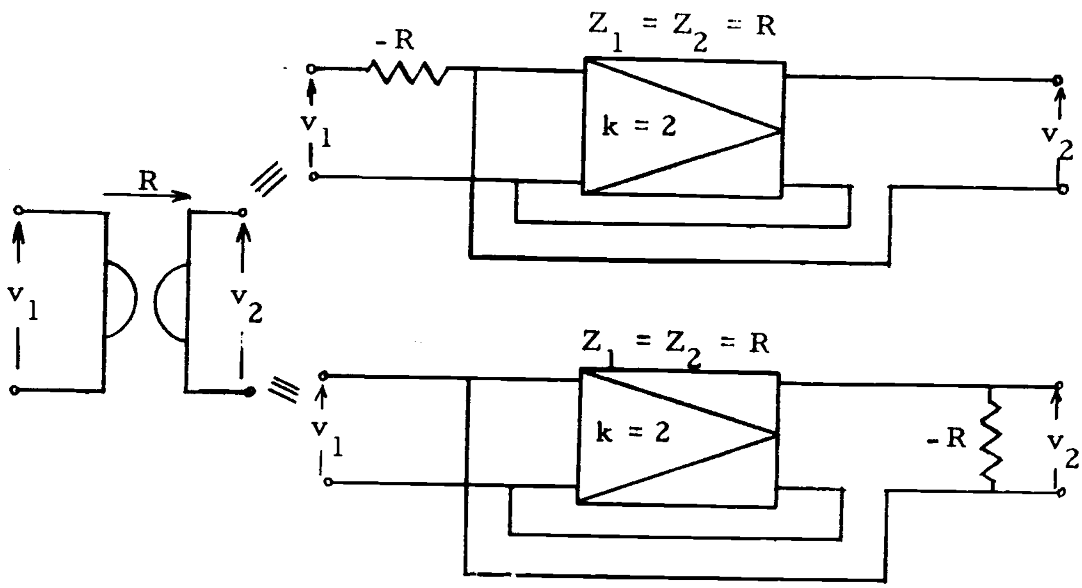

Figure 4-9. A realization of an ideal gyrator by p-s connection of the feedback circuit.

3b. Realization by Two Parallel VCCSs

The admittance matrix of the gyrator was defined as:

$$[Y] = \begin{bmatrix} 0 & \frac{1}{R} \\ -\frac{1}{R} & 0 \end{bmatrix} . \tag{4-17}$$

The admittance matrix can be partitioned into two submatrices

$$[Y] = \begin{bmatrix} 0 & \frac{1}{R} \\ 0 & 0 \end{bmatrix} + \begin{bmatrix} 0 & 0 \\ -\frac{1}{R} & 0 \end{bmatrix} . \tag{4-18}$$

Each part of the matrices can be represented by a VCCS with opposing polarities. Thus a gyrator can be realized by paralleling two VCCS with opposite polarity. The circuit is shown in Figure 4-10.

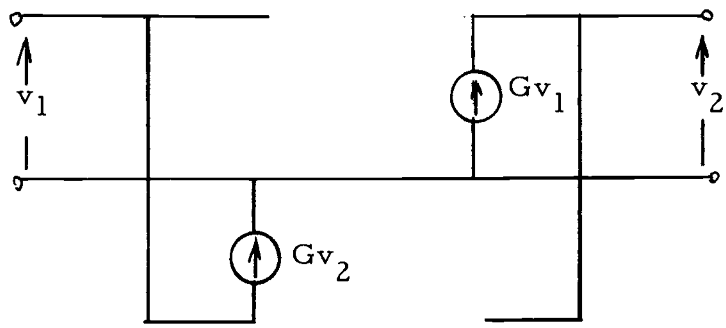

Figure 4-10. A realization of an ideal gyrator using two VCCS.

3c. Realization by Cascading NIC and NIV

Negative impedance converter (NIC) is a two port device in which the impedance seen at either port is the negative of the impedance connected to the other port. Practical NICs have two classes. One of them is the class in which the NIC reverses the current flow at one of the ports with respect to the direction of current flow at the other. Such a device is referred to as a current-inversion negative impedance converter (INIC). The following equations apply to it:

$$v_1 = v_2, \tag{4-19a}$$

$$i_1 = \frac{1}{k} i_2, \tag{4-19b}$$

where k is the gain of the NIC. Its transmission matrix is

$$[T]_{nic} = \begin{bmatrix} 1 & 0 \\ 0 & -\frac{1}{k} \end{bmatrix} . \tag{4-20}$$

The other class of NICs operates by inverting the voltage polarity while leaving the direction of current flow unchanged. The voltage inversion negative impedance converter (VNIC) is described by the following equations:

$$v_1 = -\frac{1}{k} v_2, \tag{4-21a}$$

$$i_1 = -i_2. \tag{4-21b}$$

Its transmission matrix is

$$[T]_{vnic} = \begin{bmatrix} -\frac{1}{k} & 0 \\ 0 & 1 \end{bmatrix} . \tag{4-22}$$

An ideal negative impedance inverter is a two port device in which the input impedanze Z_i is proportional to the negative of the load admittance, Y_L. In other words,

$$Z_i = -R^2 Y_L = -\frac{R^2}{Z_L} . \tag{4-23}$$

The necessary and sufficient conditions for the two port device to be an ideal NIV circuit, in terms of the Z parameters, are

$$Z_{11} = Z_{22} = 0, \tag{4-24a}$$

$$Z_{12}Z_{21} = R^2. \tag{4-24b}$$

If we choose $Z_{12} = Z_{21} = \pm R$, then its transmission matrix can be expressed as

$$[T]_{niv} = \begin{bmatrix} 0 & \pm R \\ \pm\frac{1}{R} & 0 \end{bmatrix}. \tag{4-25}$$

The circuit can be realized by using one negative resistance and two positive resistances, or two negative resistances with one positive resistance as shown in Figure 4-11:

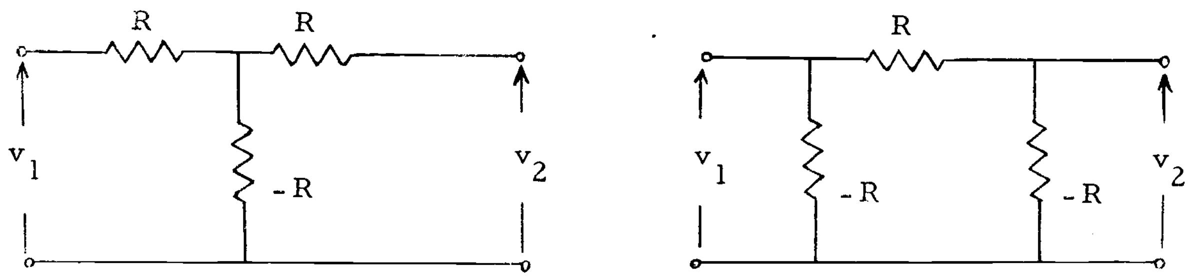

Figure 4-11. A realization of NIV by using positive and negative resistances.

When a negative impedance converter with gain $k = 1$ is cascaded with a negative impedance inverter, the transmission matrix can be represented as

$$\begin{bmatrix} \pm 1 & 0 \\ 0 & -1 \end{bmatrix} \begin{bmatrix} 0 & \pm R \\ \pm\frac{1}{R} & 0 \end{bmatrix} = \begin{bmatrix} 0 & \pm R \\ \pm\frac{1}{R} & 0 \end{bmatrix} . \tag{4-26}$$

Thus the gyrator can be realized by cascading an NIC and an NIV:

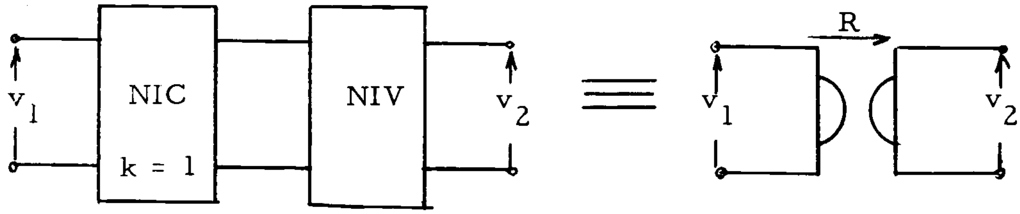

Figure 4-12. A realization of the gyrator by cascading NIC and NIV.

3d. Experimental Results of the Gyrator

The design of an actual gyrator circuit is based on cascading an INIC and an NIV. The INIC and NIV are realized by using operational amplifiers. An ideal operational amplifier is an ideal voltage amplifier of very low output impedance, very high input impedance and very high gain, with the property that the output voltage is proportional to the difference in the voltages applied to the two input terminals. An equivalent circuit is shown in Figure 4-13:

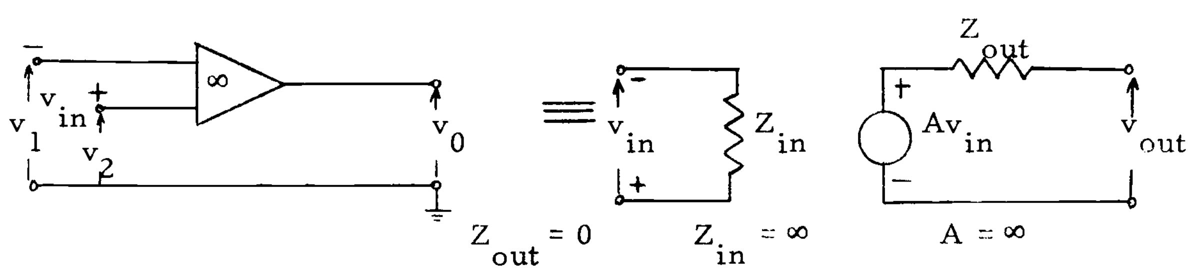

Figure 4-13. An equivalent circuit of an ideal operational amplifier.

The two summing point constraints are very important and defined as:

i) No current flows into either input terminal of the ideal operational.

ii) When negative feedback is applied around the ideal operational amplifier, the voltage between the input terminals approaches zero.

These two statements are used to analyze various circuits. The INIC and NIV are realized using the two constraints. As an example, consider the circuit of Figure 4-14. By directly applying the two constraints, the following relations result.

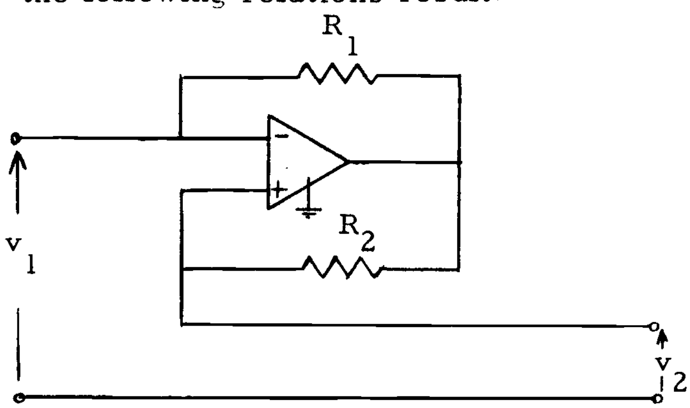

Figure 4-14. An INIC realization by using operational amplifier.

$$\begin{bmatrix} v_1 \\ i_1 \end{bmatrix} = \begin{bmatrix} 1 & 0 \\ 0 & -\frac{R_2}{R_1} \end{bmatrix} \begin{bmatrix} v_2 \\ -I_2 \end{bmatrix} . \tag{4-27}$$

By comparing the transmission matrix with Equation (4-20), it is obvious that the circuit is an INIC with $k = R_1/R_2$. For the NIV circuit consider the circuit of Figure 4-15.

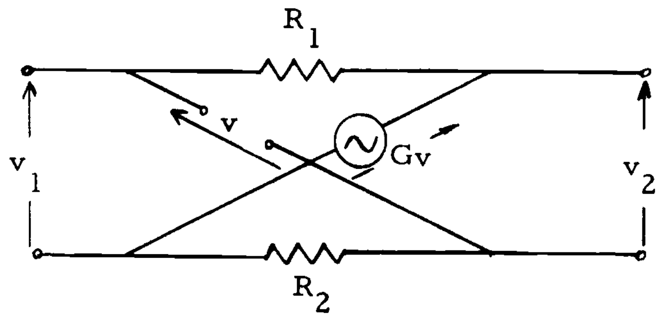

Figure 4-15. The NIV circuit.

This is a circuit replacing a current controlled current source by a voltage controlled voltage source in an NIV circuit which was given by Lundry (10). Analyzing the circuit, the transmission matrix is found to be

$$[T]_{NIV} = \begin{bmatrix} \frac{1}{G} & \frac{R_2(G+1)}{G} \\ -\frac{G-1}{GR_1} & \frac{R_2}{GR_1} \end{bmatrix}. \qquad (4\text{-}28)$$

When $|G| \gg 1$, the transmission matrix reduces to

$$[T]_{NIV} = \begin{bmatrix} 0 & R_2 \\ -\frac{1}{R_1} & 0 \end{bmatrix}. \qquad (4\text{-}29)$$

Since the operational amplifier is a VCVS with the gain $|G| \gg 1$, the NIV can be formed by replacing the VCVS by the operational amplifier.

The resulting circuit is shown in Figure 4-16. Clearly, the gyrator can be easily formed by using two operational amplifiers.

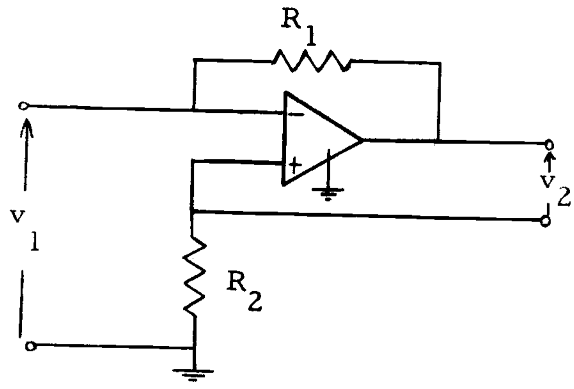

Figure 4-16. The NIV circuit using operational amplifier.

An actual gyrator circuit was made and tested. Two NEXUS SQ-10a operational amplifers, with a dc gain of 100, 000 and a 2MHz cut off frequency, were used in the experiment. Figure 4-17 shows the circuit.

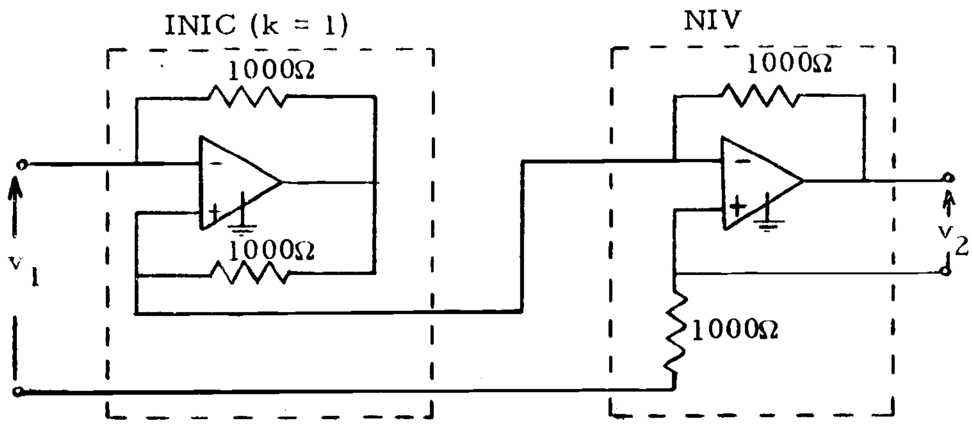

Figure 4-17. The gyrator circuit using operational amplifier.

The experimental results are shown in the following curves and oscillograms.

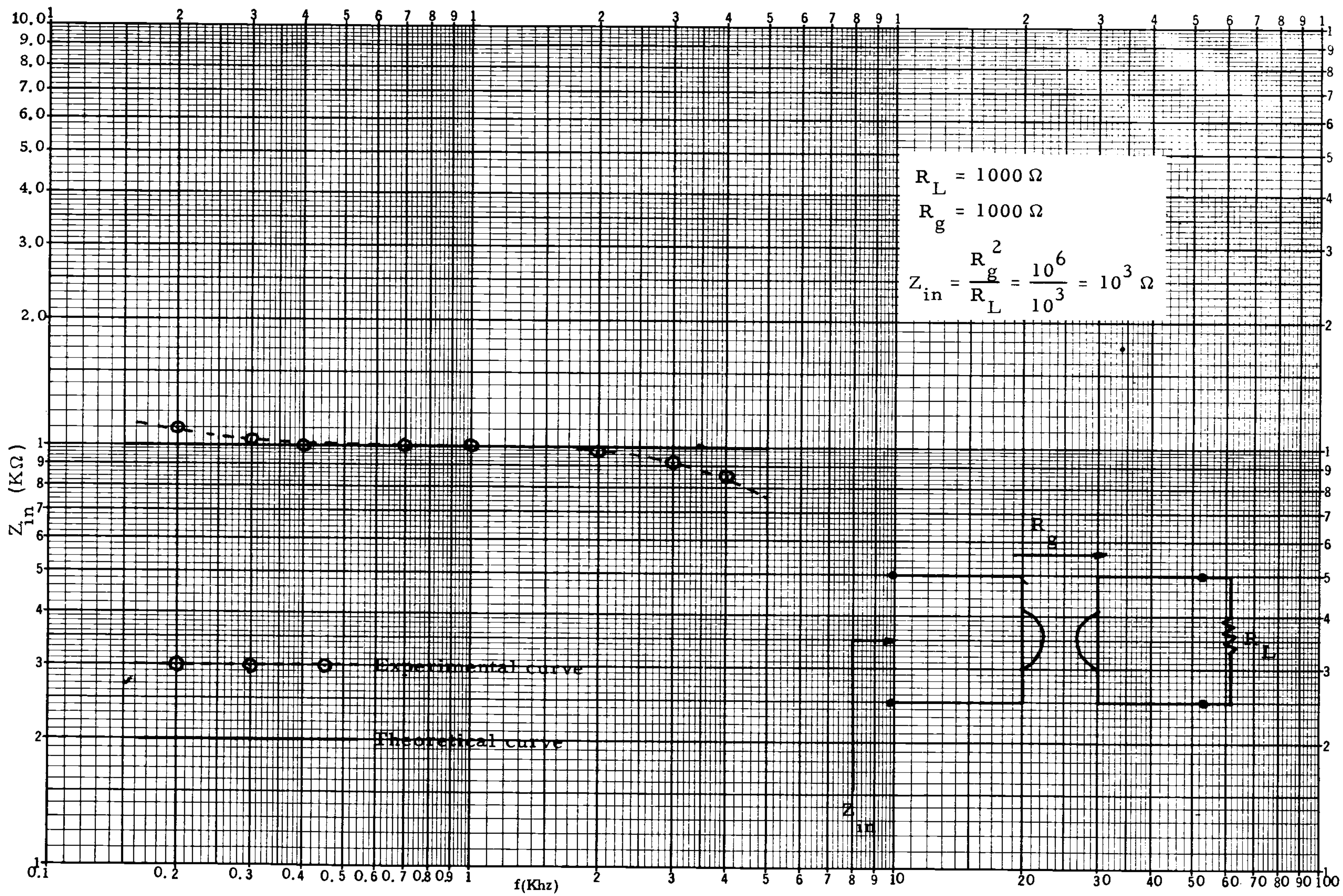

Figure 4-18. Input impedance characteristic of the resistively terminate gyrator.

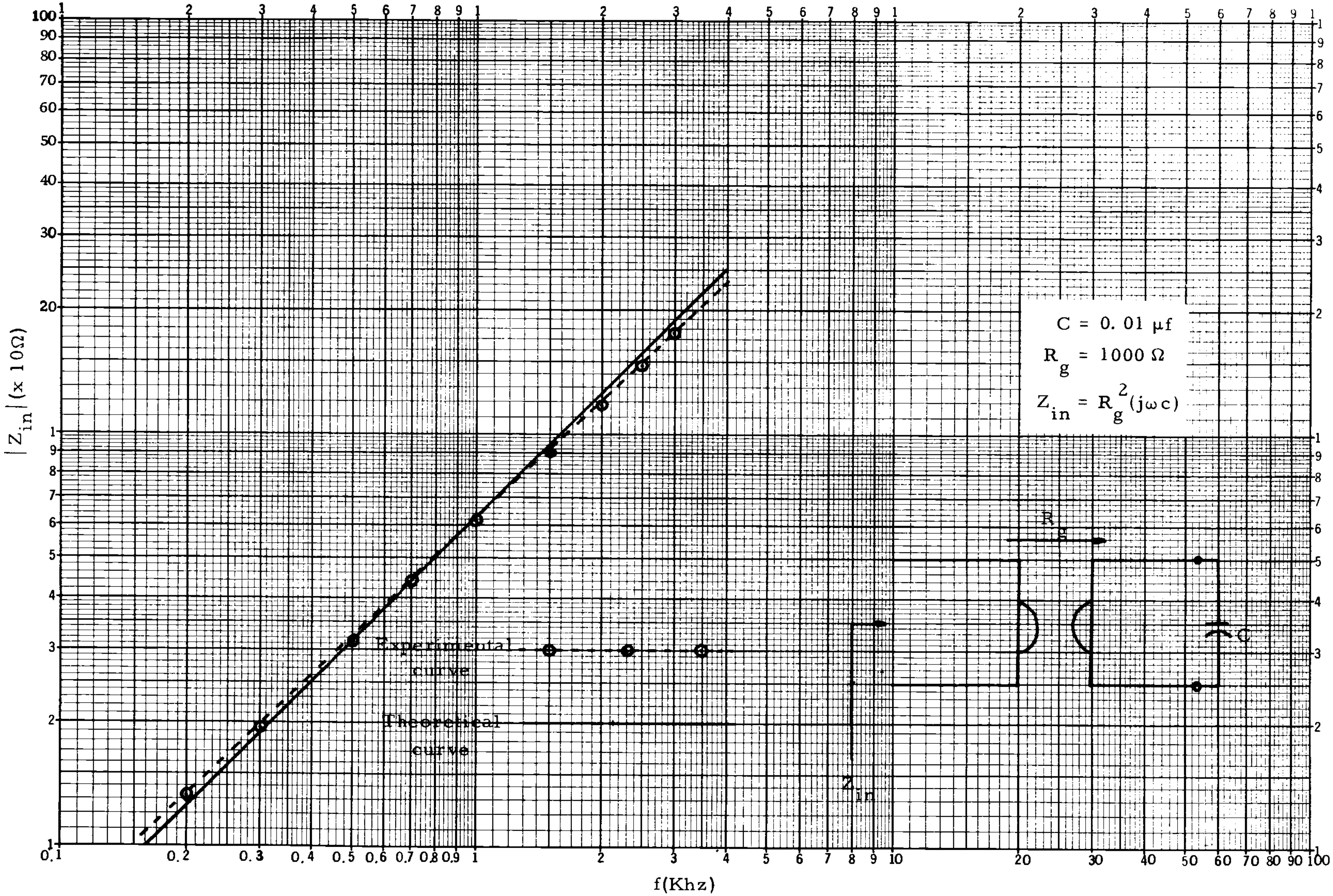

Figure 4-19. Input impedance characteristic of capacitively terminated gyrator

Figures 4-18 and 4-19 are plots of the impedance, Z_{in}, vs the frequency, f, when the gyrator is terminated with a resistance R_L or a capacitance. The curves show that the input impedance agrees closely with theoretical results at frequencies between 250 Hertz to 2500 Hertz. Oscillograms 1 through 4 show the phase difference between a resistance and the simulated inductor L (see Figures 4-20 and 4-21) at the frequency f = 500, 1000, 2000, 2500 Hertz.

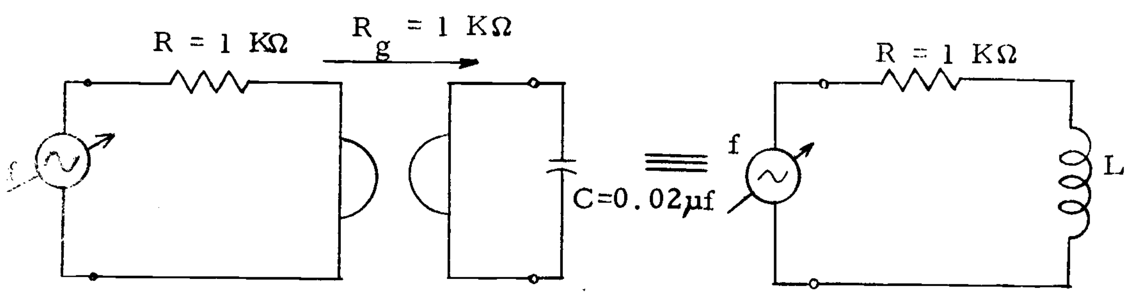

f = 500, 1000, 2000, 2500 Hertz $L = R_g^2 C = 0.02$ h

Figure 4-20. Simulated R-L circuit.

Phase difference $\theta = \sin^{-1} \frac{b}{a}$

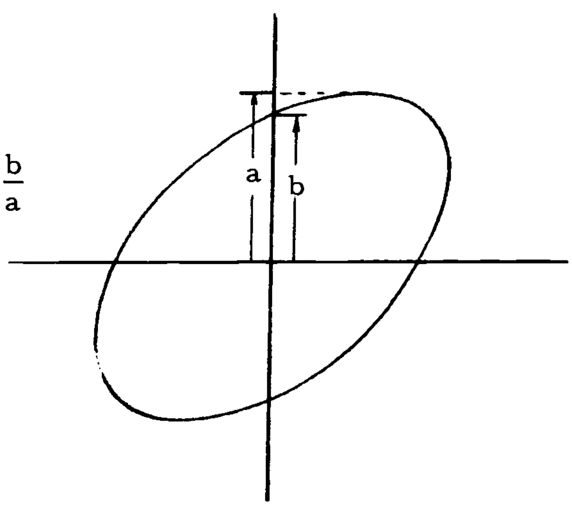

Figure 4-21. Phase-difference pattern.

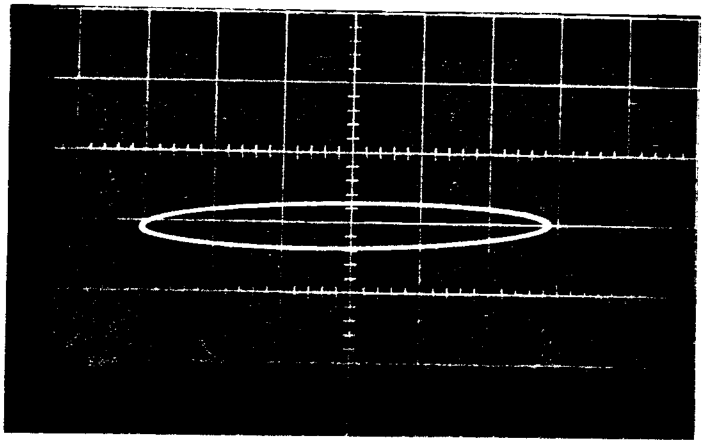

Oscillogram # 1

f = 500 c/s

Phase difference
(theoretical) $\theta = 86.42^\circ$
(experimental) $\theta \approx 87^\circ$

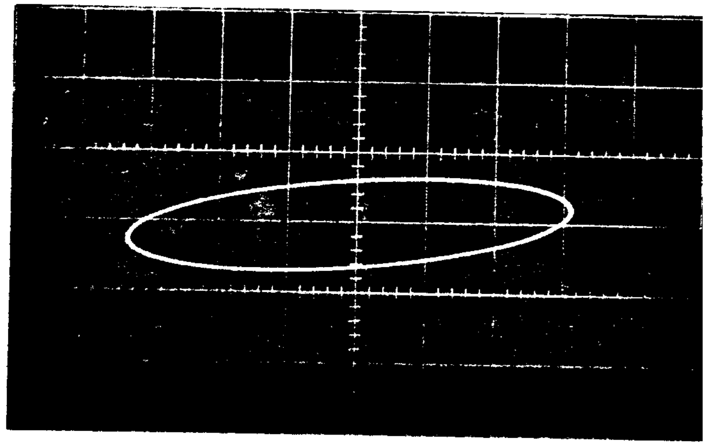

Oscillogram # 2

f = 1000 c/s

$\theta = 82.84^\circ$
$\theta \approx 82^\circ$

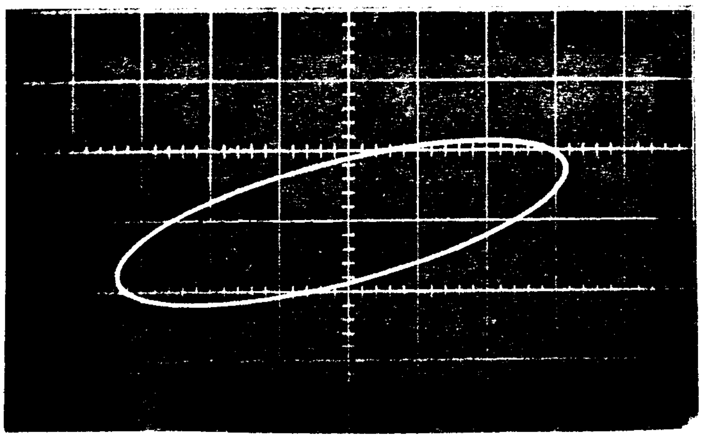

Oscillogram # 3

f = 2000 c/s

Phase difference
(theoretical) $\theta = 75.45^\circ$
(experimental) $\theta \approx 70^\circ$

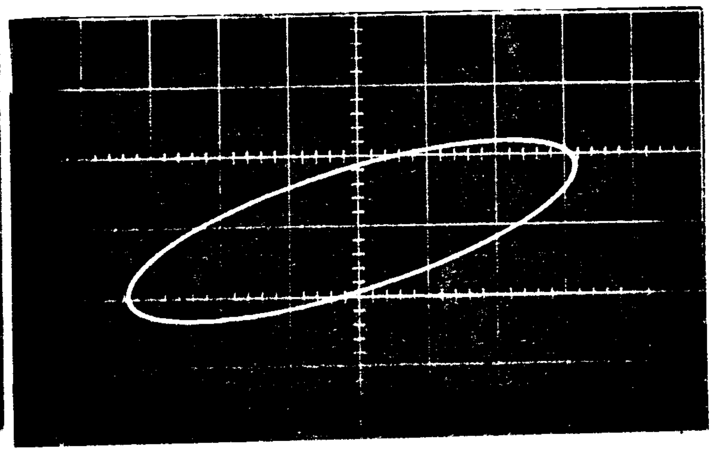

Oscillogram # 4

f = 2500 c/s

$\theta = 71.7^\circ$
$\theta \approx 60^\circ$

V. ACTIVE FILTER SYNTHESIS USING GYRATOR

In the design of low frequency circuits, inductance, if required, is usually needed in large values. Consequently, the physical realization of these inductances becomes very impractical, because of size and cost limitations, and because of resistive losses. In addition, when precise specifications are to be attained, conventional circuits with inductances can not be used, because of the inherent resistance of inductors. On the other hand, capacitances of large values can be obtained with low loss and for a reasonable cost. Thus, the use of networks containing only resistors and capacitors are to be considered. The natural frequencies of passive RC networks are restricted to the negative real axis of the complex frequency plane, and the natural frequencies must be simple, i.e., of the first order. It is therefore not possible to obtain the complex natural frequencies. However, the situation can be improved by using active elements. The most frequently encountered active elements are controlled sources, negative impedance converters and gyrators. Each active element had its advantages and disadvantages. The realization of the gyrator has been discussed in Chapter IV. In this chapter we shall apply the sensitivity minimization techniques, which have been described in Chapter III, to RC-gyrator synthesis.

1. Direct Design Method

The simplest and most direct way to design active filters using gyrators is to first design the conventional L-C filter, and then replace all the inductors with gyrators and capacitors. As an example, a 3-pole maximumally-flat low pass transfer function can be realized using the following procedures:

i) Find the pole locations.

$$s_1 = e^{j\frac{2}{3}\pi} = -0.5 + j0.866$$

$$s_2 = e^{j\pi} = -1 + j0$$

$$s_3 = e^{j\frac{4}{3}\pi} = -0.5 - j0.866.$$

ii) Construct the transfer function

$$Z_{21} = \frac{H}{(s+0.5-j0.866)(s+1)(s+0.5+j0.866)}$$

$$= \frac{H}{s^3+2s^2+2s+1} \quad . \tag{5-1}$$

iii) Design the network as an LC filter loaded with unity resistance.

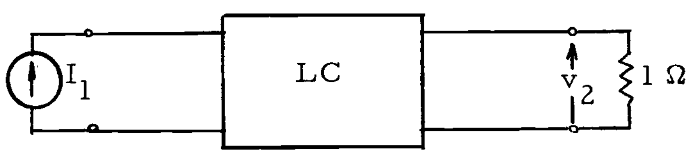

Figure 5-1. LC network terminated with unity resistance.

The transfer impedance Z_{21} can be expressed by open circuit parameters:

$$Z_{12} = \frac{z_{21}}{1+z_{22}} . \tag{5-2}$$

iv) Assign z_{21} and z_{22}

$$Z_{12} = \frac{H}{s^3+2s^2+2s+1} = \frac{\dfrac{H}{s^3+2s}}{1+\dfrac{2s^2+1}{s^3+2s}}$$

$$= \frac{z_{12}}{1+z_{22}} .$$

Thus,

$$z_{12} = \frac{H}{s^3+2s} , \tag{5-3a}$$

and

$$z_{22} = \frac{2s^2+1}{s^3+2s} . \tag{5-3b}$$

v) Synthesize the network.

Since all zeros of z_{12} lie at $s = \infty$, the desired network is obtained through the continued-fraction development of z_{22}

$$z_{22} = \cfrac{1}{\cfrac{3}{2}+\cfrac{1}{\cfrac{4}{3}s+\cfrac{1}{\cfrac{3}{2}s}}} . \tag{5. 4}$$

The realized network is shown in Figure 5-2.

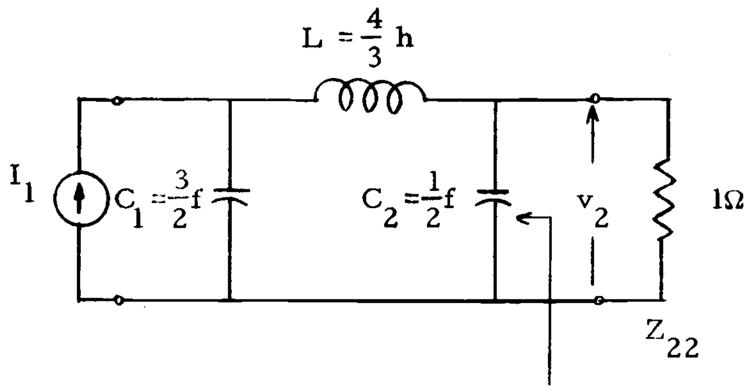

Figure 5-2. The realized network of Equation (5-1).

vi) Denormalize the element values in terms of the given specification.

Suppose we wish to increase the impedance level to k_z, and scale the frequency to k_f, the denormalized values R^*, L^* and C^* are changed to

$$R^* = k_z R \tag{5-5a}$$

$$L^* = \frac{k_z}{k_f} L \tag{5-5b}$$

$$C^* = \frac{1}{k_z k_f} C \tag{5-5c}$$

vii) Replace the inductor by two gyrators and a capacitor

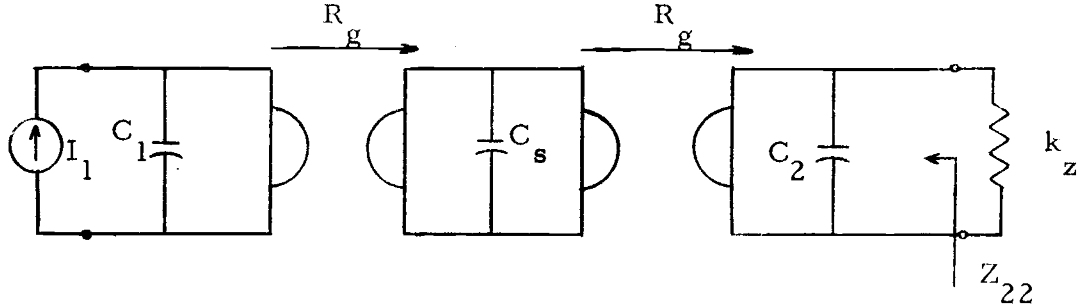

Figure 5-3. Replacing the inductance in Figure 5-2 by gyrators.

Where

$$C_1 = \frac{3}{2} \frac{1}{k_z k_f} , \tag{5-6a}$$

$$C_2 = \frac{1}{2} \frac{1}{k_z k_f} , \tag{5-6b}$$

$$C_s = \frac{L}{R_g^2} = \frac{4}{3} \frac{1}{R_g^2} \frac{k_z}{k_f} . \tag{5-6c}$$

The active filter design using this direct method is quite simple, the simulated inductor is $L = R_g^2 C_s$. If, under certain conditions R_g drifts, then an accurate L cannot be attained; therefore, the characteristic of the transfer function will be changed. An example of a second degree low pass filter will be used to examine this change. The transfer function is

$$G_{12} = \frac{1}{s^2 + 2\xi s + 1} . \tag{5-7}$$

Applying the previous procedure, the network can be found as follows:

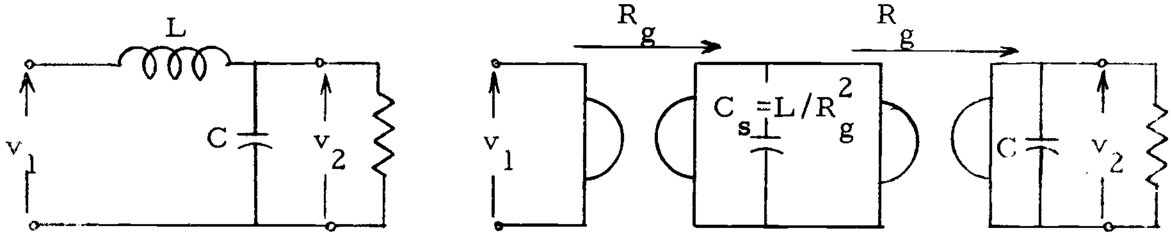

Figure 5-4. The realized network of Equation (5-7).

where

$$L = 2\xi \tag{5-8a}$$

$$C = \frac{1}{2\xi} \tag{5-8b}$$

$$R = 1 \tag{5-8c}$$

and

$$C_s = \frac{R_g^2}{L} \tag{5-8d}$$

Denormalize each circuit element by changing the impedance level to R_z and the frequency scale to ω_o. Then the element values become

$$L^* = \frac{2\xi R_z}{\omega_o}, \tag{5-9a}$$

$$C^* = \frac{1}{2\xi\omega_o R_z}, \tag{5-9b}$$

and

$$R^* = R_z. \tag{5-9c}$$

If the gyration resistance R_g is varied to R'_g the simulated inductance is changed to

$$L' = L\left(\frac{R'_g}{R_g}\right)^2 = La^2, \tag{5-10}$$

where

$$a = \frac{R'_g}{R_g}. \tag{5-11}$$

The denormalized transfer function of Figure 5-4 becomes

$$G_{12}(s) = \frac{\frac{1}{LC}}{s^2 + \frac{1}{CR}s + \frac{1}{LC}}$$

$$= \frac{\omega_o^2}{s^2 + 2\xi\omega_o s + \omega_o^2} \qquad (5\text{-}12)$$

When the gyration resistance is changed the simulated inductance changes to L'. The transfer function thus becomes

$$G_{12}(s) = \frac{(\frac{\omega_o}{a})^2}{s^2 + 2\xi\, a(\frac{\omega_o}{a}) + (\frac{\omega_o}{a})^2}$$

$$= \frac{\omega_n^2}{s^2 + 2\xi_n\omega_n + \omega_n^2} \qquad (5\text{-}13)$$

The dc gain remains unity, but the damping ratio ξ_o and the resonant frequency ω_o are changed to ξ_n and ω_n, respectively.

$$\omega_n = \frac{\omega_o}{a} = \omega_o(\frac{R_g}{R'_g}), \qquad (5\text{-}14a)$$

and

$$\xi_n = \xi \cdot a = \xi(\frac{R'_g}{R_g}), \qquad (5\text{-}14b)$$

Figure 5-5 shows the percent change in damping ratio with percent change in R_g. Figure 5-6 shows the percent change in resonant frequency with percent change in R_g.

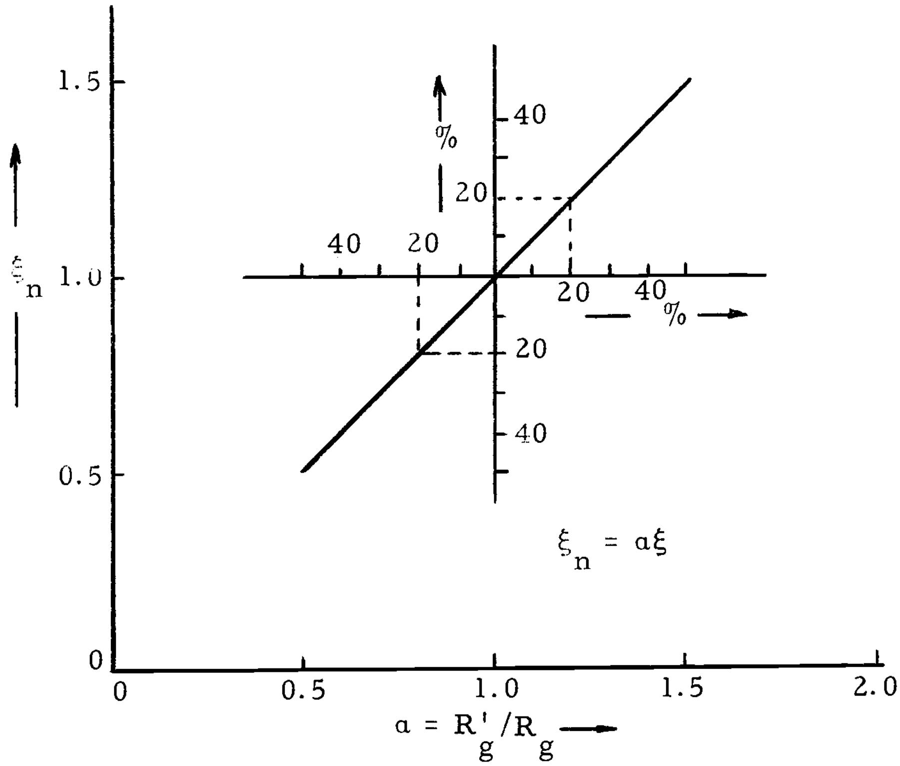

Figure 5-5. Damping ratio vs a for direct design method.

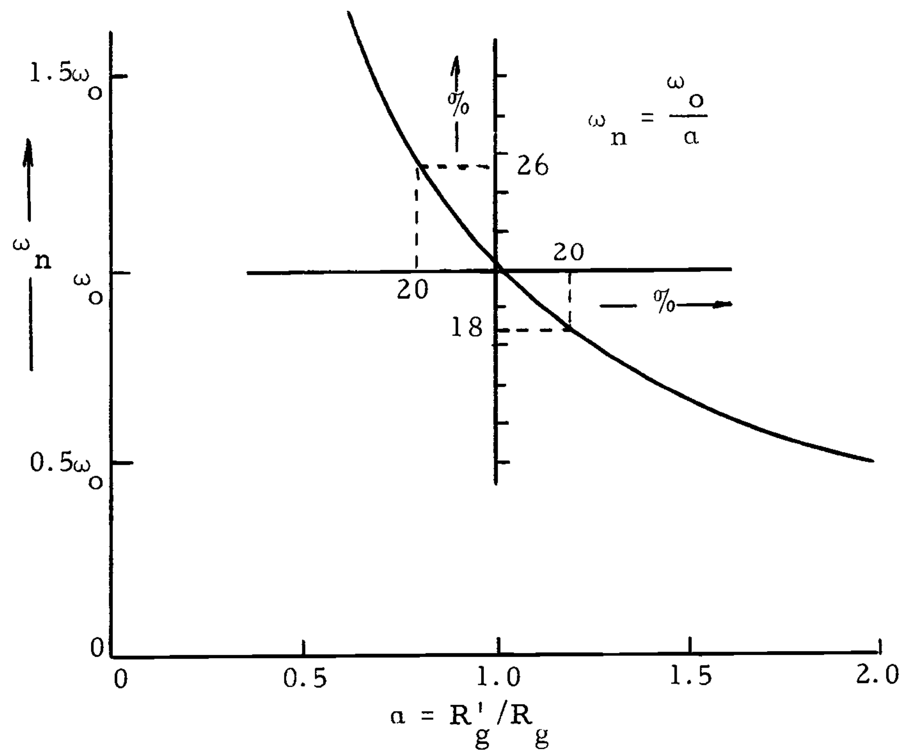

Figure 5-6. Resonant frequency vs a for direct design method.

From Figures 5-5 and 5-6, we observe that when the gyration resistance is increased by 10%, the damping ratio ξ_n and resonant frequency ω_n vary 10% and 9%, respectively. This will be compared with the other methods later.

2. Single Gyrator Design Method

Although the direct design method is quite simple, it has the disadvantages that pole locations of the transfer function are sensitive to the change of gyration resistance, and the network needs more than one gyrator. There is a better method using a single gyrator cascaded by passive networks at both ports as shown in Figure 5-7 (13).

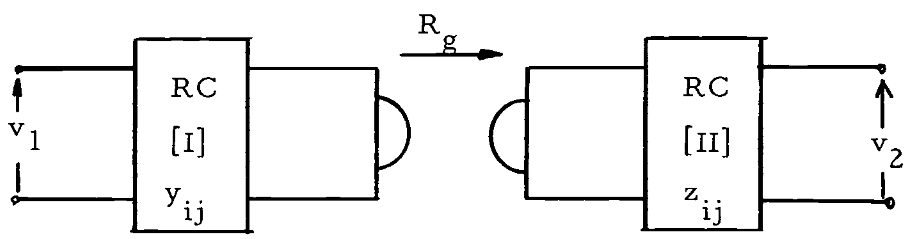

Figure 5-7. A gyrator cascaded with two RC networks.

Let network I in Figure 5-7 be defined by its y-parameters $y_{ij}^{(I)}$, and the network II be defined by its z-parameter $z_{ij}^{(II)}$. Then the open-circuit voltage transfer function for the overall network is

$$G_{12}(s) = \frac{V_2(s)}{V_1(s)} = \frac{N(s)}{D(s)} = -\frac{R_g y_{12}(s) z_{12}(s)}{z_{11}(s)+R_g^2 y_{22}(s)} = -\frac{G y_{21}(s) z_{21}(s)}{y_{22}(s)+G^2 z_{11}(s)}. \tag{5-15}$$

Divide both denominator and numerator by an arbitrary polynomial $Q(s)$ and decompose $D(s)/Q(s)$ into the form of $z_{11}(s)+R_g^2 y_{22}(s)$. Thus

$$\frac{D(s)}{Q(s)} = \frac{D_2(s)}{Q_2(s)} + R_g^2 \frac{D_1(s)}{Q_1(s)} = \frac{D_2(s)Q_1(s)+R_g^2 D_1(s)Q_2(s)}{Q_1(s)Q_2(s)}. \tag{5-16}$$

Therefore

$$z_{11} = \frac{D_2(s)}{Q_2(s)}, \quad y_{22} = \frac{D_1(s)}{Q_1(s)}, \tag{5-17}$$

$$Q(s) = Q_1(s)Q_2(s), \tag{5-18a}$$

$$D(s) = D_2(s)Q_1(s) + R_g^2 D_1(s)Q_2(s). \tag{5-18b}$$

The decomposition may be achieved by using optimum polynomial techniques proposed by Calahan which have been summarized in Chapter III. The first way, denoted by (A), is the optimum non-unique decomposition. The second, denoted latter by (B), is the optimum unique decomposition.

(A). The optimum non-unique decomposition has the form of

$$D(s) = A_{on} \prod_{1}^{n/2} (s+a_i)^2 + B_{on} \prod_{1}^{n/2} (s+b_i)^2. \tag{5-19}$$

Consider a low pass filter with the transfer function of

$$G_{12}(s) = \frac{H_o \omega_o^2}{s^2 + 2\xi\omega_o s + \omega_o^2} = \frac{N(s)}{D(s)} . \tag{5-20}$$

D(s) has an optimum decomposition of the form

$$D(s) = s^2 + 2\xi\omega_o s + \omega_o^2 = A_{on}(s+a)^2 + B_{on}(s+b)^2 . \tag{5. 20'}$$

By equating the corresponding coefficients

$$A_{on} + B_{on} = 1, \tag{5-21a}$$

$$A_{on} a + B_{on} b = \xi\omega_o , \tag{5-21b}$$

and

$$A_{on} a^2 + B_{on} b^2 = \omega_o^2 . \tag{5-21c}$$

There are four unknowns and only three equations available, so we shall make some assumptions. By calculations we find that

$$A_{on} = \frac{1}{1 + B_{on}/A_{on}} . \tag{5-22}$$

Arbitrarily select

$$B_{on}/A_{on} = n^2 , \tag{5-23}$$

then

$$A_{on} = \frac{1}{1+n^2} , \quad \text{and} \quad B_{on} = \frac{n^2}{1+n^2} , \tag{5-24}$$

Substituting Equations (5-23) and (5-24) into Equations (5-21a, b and c) yields

$$a = \omega_o(\xi + n\sqrt{1-\xi^2}) \tag{5-25a}$$

$$b = \omega_o(\xi - \frac{1}{n}\sqrt{1-\xi^2}) \tag{5-25b}$$

From Equations (5-20) and (5-18b)

$$D_2(s)Q_1(s) = A_{on}(s+a)^2, \tag{5-26}$$

$$D_1(s)Q_2(s) = \frac{1}{R_g^2}[B_{on}(s+b)^2]. \tag{5-27}$$

Assign

$$D_1 = k_o \frac{B_{on}}{R_g^2}(s+b), \tag{5-28a}$$

$$Q_2 = \frac{1}{k_o}(s+b), \tag{5-28b}$$

$$D_2 = A_{on}(s+a), \tag{5-28c}$$

and

$$Q_1 = (s+a), \tag{5-28d}$$

where k_o is impedance scaling factor.

Then

$$z_{11} = \frac{D_2(s)}{Q_2(s)} = k_o A_{on} \frac{s+a}{s+b}, \tag{5-29a}$$

and

$$y_{22} = \frac{D_1(s)}{Q_1(s)} = \frac{k_o B_{on}}{R_g^2} \frac{s+b}{s+a}. \tag{5-29b}$$

y_{12} and z_{12} can be found from the numerator:

$$\frac{N(s)}{Q(s)} = \frac{H_o \omega_o^2 k_o}{(s+a)(s+b)} = -R_g y_{12}(s) z_{12}(s). \tag{5-30}$$

Now assign

$$-y_{12}(s) = k_o \frac{X_1}{s+a}, \tag{5-31a}$$

and

$$z_{12}(s) = k_o \frac{X_2}{s+b}, \tag{5-31b}$$

where

$$X_1 X_2 = \frac{H_o \omega_o^2}{k_o R_g^2}. \tag{5-32}$$

From Equations (5-29b) and (5-31a), the RC network at the left port of the gyrator can be realized and shown as in Figure 5-8. The continued-fractional expansion of y_{22} takes the form of Figure 5-8.

$$y_{22} = \cfrac{1}{\cfrac{R_g^2}{k_o B_{on}} + \cfrac{1}{\cfrac{k_o B_{on}}{R_g^2 (a-b)} s + \cfrac{1}{\cfrac{R_g^2}{k_o B_{on}} - \cfrac{a-b}{b}}}} \tag{5-33}$$

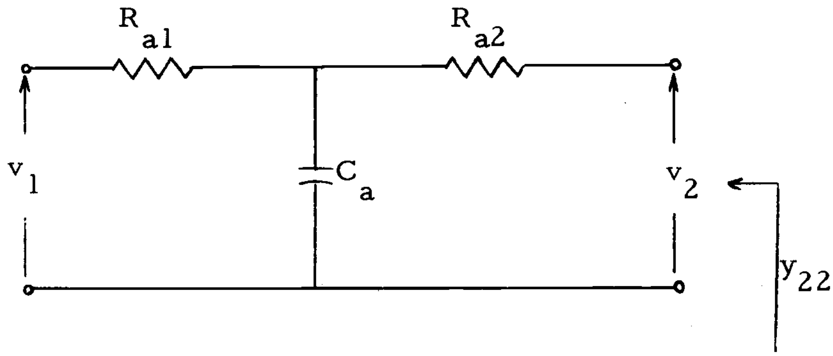

Figure 5-8. The RC network at the left port of the gyrator.

where

$$R_{a1} = \frac{R_g^2(a-b)}{k_o B_{on} b}, \qquad R_{a2} = \frac{R_g^2}{k_o B_{on}},$$

$$C_a = \frac{k_o B_{on}}{R_g^2(a-b)}, \qquad X_1 = \frac{bB_{on}}{R_g^2} \tag{5-34}$$

Similarly, the RC network at the right of the gyrator is realized by Equations (5-29a) and (5-31b), which yields Equation (5-35) and Figure 5-9.

$$z_{11} = \cfrac{1}{k_o A_{on} + \cfrac{1}{\cfrac{1}{k_o A_{on}(a-b)} s + \cfrac{1}{\frac{1}{b}[k_o A_{on}(a-b)]}}} \tag{5-35}$$

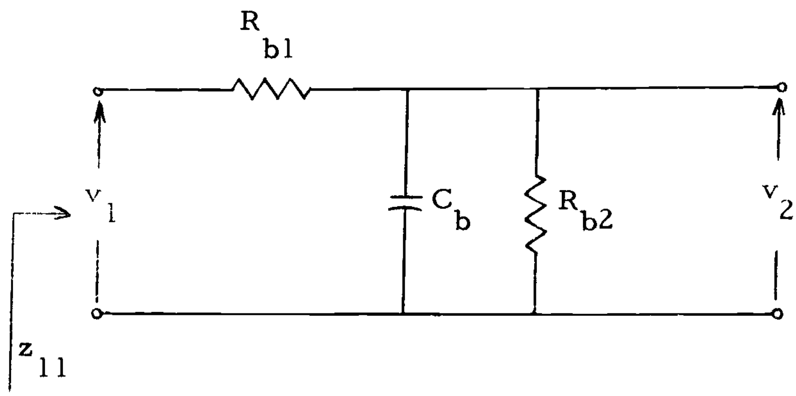

Figure 5-9. The RC network at the right port of the gyrator.

where

$$R_{b1} = k_o A_{on}, \qquad R_{b2} = \frac{1}{b}\,[k_o A_{on}(a-b)],$$
$$C_b = \frac{1}{k_o A_{on}(a-b)}, \qquad X_2 = B_{on}(a-b)\,. \tag{5-36}$$

The complete network is shown in Figure 5-10.

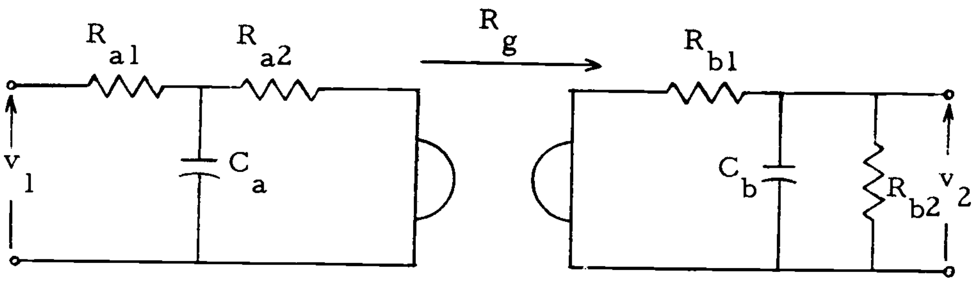

Figure 5-10. The realization of Equation (5-20).

Substituting the values of a, b, A_{on} and B_{on} into R_{a1}, R_{a2}, R_{b1}, R_{b2}, C_a and C_b yields

$$R_{a1} = \frac{(1+n^2)^2}{n^3}\,\frac{R_g^2}{k_o}\,\frac{\sqrt{1-\xi^2}}{\xi - \frac{1}{n}\sqrt{1-\xi^2}}, \qquad R_{a2} = \frac{1+n^2}{n^2}\,\frac{R_g^2}{k_o},$$

$$R_{b1} = \frac{1}{1+n^2}\,k_o, \qquad R_{b2} = \frac{1}{n}\,k_o\,\frac{\sqrt{1-\xi^2}}{\xi\,\frac{1}{n}\sqrt{1-\xi^2}}, \tag{5-37}$$

$$C_a = \frac{n^3}{(1+n^2)^2}\,\frac{k_o}{R_g^2\,\omega_o}\,\frac{1}{\sqrt{1-\xi^2}}, \qquad C_b = n\,\frac{1}{k_o\,\omega_o\sqrt{1-\xi^2}}\,.$$

It is instructive to examine the characteristic change of the transfer function due to the change of gyration resistance. The transfer function of the network designed by this method (Figure 5-10) is

$$G_{12}(s) = -\frac{R_g y_{12}(s) z_{12}(s)}{z_{11}(s) + R_g^2 y_{22}(s)}$$

$$= \frac{\frac{1}{R_g} k_o b(a-b) A_{on} B_{on}}{s^2(A_{on}+B_{on}) + 2s(aA_{on}+bB_{on}) + a^2 A_{on} + b^2 B_{on}}$$

$$= \frac{\omega_o^2\left[\frac{1}{R_g} k_o \sqrt{1-\xi^2}\left(\xi - \frac{1}{n}\sqrt{1-\xi^2}\right) \frac{n}{n^2+1}\right]}{s^2 + 2\xi\omega_o s + \omega_o^2}$$

$$= \frac{H_o \omega_o^2}{s^2 + 2\xi\omega_o s + \omega_o^2} \quad , \tag{5-38}$$

where

$$H_o = \frac{1}{R_g} k_o \sqrt{1-\xi^2}\left(\xi - \frac{1}{n}\sqrt{1-\xi^2}\right) \frac{n}{n^2+1} \quad . \tag{5-39}$$

When the gyration resistance changes from R_g to R_g' letting $\alpha = \frac{R_g'}{R_g}$ as before, we obtain

$$G_{12}(s) = -\frac{\alpha R_g y_{12}(s) z_{12}(s)}{z_{11}(s) + \alpha^2 R_g^2 y_{22}(s)}$$

$$= \frac{\frac{1}{R_g} k_o b B_{on} A_{on}(a-b)}{s^2\left(\frac{A_{on}}{\alpha} + \alpha B_{on}\right) + 2\left(\frac{aA_{on}}{\alpha} + bB_{on}\alpha\right)s + \frac{A_{on}a^2}{\alpha} + \alpha B_{on} b^2}$$

$$= \frac{\frac{1}{R_g} k_o b B_{on} A_{on} (a-b)}{Y_1 s^2 + a Y_2 \xi \omega_o s + \omega_o^2 Y_3}$$

$$= \frac{\frac{1}{R_g} \frac{1}{Y_1} k_o b B_{on} A_{on} (a-b)}{s^2 + (\frac{Y_2}{Y_1})\, 2\xi\omega_o s + (\frac{Y_3}{Y_1})\omega_o^2}$$

$$= \frac{\frac{1}{Y_1}\left[\frac{1}{R_g}\left(\omega_o^2 k_o \sqrt{1-\xi^2}(\xi - \frac{1}{n}\sqrt{1-\xi^2})\, \frac{n}{n^2+1}\right)\right.}{s^2 + (\frac{Y_2}{Y_1}) 2\xi\omega_o s + (\frac{Y_3}{Y_1})\omega_o^2}$$

$$= \frac{H_n \omega_n^2}{s^2 + 2\xi_n \omega_n s + \omega_n^2} \quad . \tag{5-40}$$

The dc gain H_o, the damping ratio ξ_o, and the resonant frequency ω_o are changed to H_n, ξ_n and ω_n, respectively. Thus

$$H_n = H_o \frac{\omega_o^2}{\omega_n^2} \frac{1}{Y_1} = H_o \frac{1}{Y_3} , \tag{5-41a}$$

$$\xi_n = \frac{Y_2}{\sqrt{Y_3 Y_1}} \xi , \tag{5-41b}$$

and

$$\omega_n = \sqrt{\frac{Y_3}{Y_1}}\, \omega_o , \tag{5-41c}$$

where

$$Y_1 = \frac{A_{on}}{a} + a B_{on} = \frac{1+n^2 a^2}{a(n^2+1)} , \tag{5-42a}$$

$$Y_2 = \frac{1}{\xi\omega_o}\left(\frac{a}{\alpha}k_1+\alpha bk_2\right) = \frac{1}{\xi\alpha(n^2+1)}\left[\xi+n\sqrt{1-\xi^2}+n^2\left(\xi-\frac{1}{n}\sqrt{1-\xi^2}\right)\right] \tag{5-42b}$$

and

$$Y_3 = \frac{1}{\omega_o^2}\left(\frac{k_1}{\alpha}a^2+\alpha k_2 b^2\right)$$

$$= \frac{1}{(n^2+1)\alpha}\left\{(1-\alpha^2)[\xi^2(1-n^2)+2n\xi\sqrt{1-\xi^2}]+n^2+\alpha^2\right\}. \tag{5-42c}$$

Substituting Equations (5-42a, b, c) into Equations (5-41a, b, c) yields

$$\omega_n = \omega_o\sqrt{\frac{(1-\alpha^2)[\xi^2(1-n^2)+2n\xi\sqrt{1-\xi^2}]+n^2+\alpha^2}{1+n^2\alpha^2}}, \tag{5-43a}$$

$$\xi_n = \frac{\xi+n\sqrt{1-\xi^2}+n^2\alpha^2\left(\xi-\frac{1}{n}\sqrt{1-\xi^2}\right)}{\sqrt{(1+n^2\alpha^2)[\xi^2(1-n^2)+2n\xi\sqrt{1-\xi^2}](1-\alpha^2)+n^2+\alpha^2}}, \tag{5-43b}$$

and

$$H_n = H_o\frac{(n^2+1)\alpha}{(1-\alpha^2)[\xi^2(1-n^2)+2n\xi\sqrt{1-\xi^2}]+n^2+\alpha^2}. \tag{5-43c}$$

Figure 5-11 shows the percent change in the damping ratio ξ_n, with percent change in R_g. Figure 5-12 shows the percent change in resonant frequency ω_n, with percent change in R_g. Figure 5-13 shows the percent change in the dc gain H_n, with percent change in R_g. Figures 5-11, 5-12, and 5-13 show the percent change of ξ_n, ω_n, H_n due to the percent change in the gyration resistance R_g. This method is based on minimum sensitivity polynomial decompsotion. This method should have a lower sensitivity than the direct design

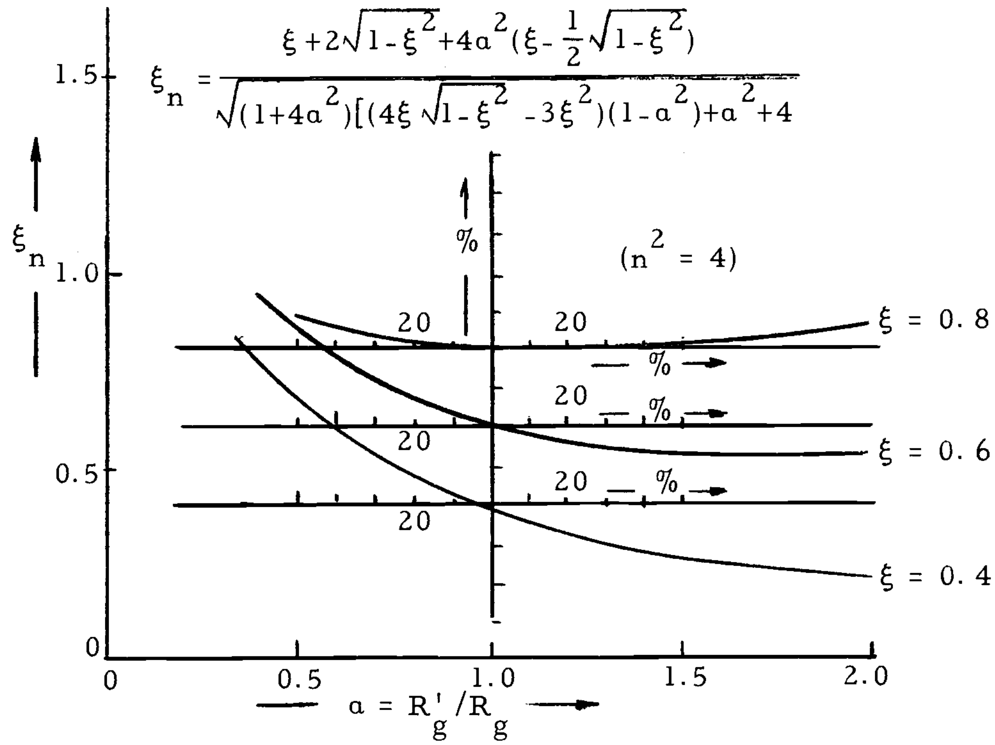

Figure 5-11. Damping ratio vs a for single gyrator design method (A).

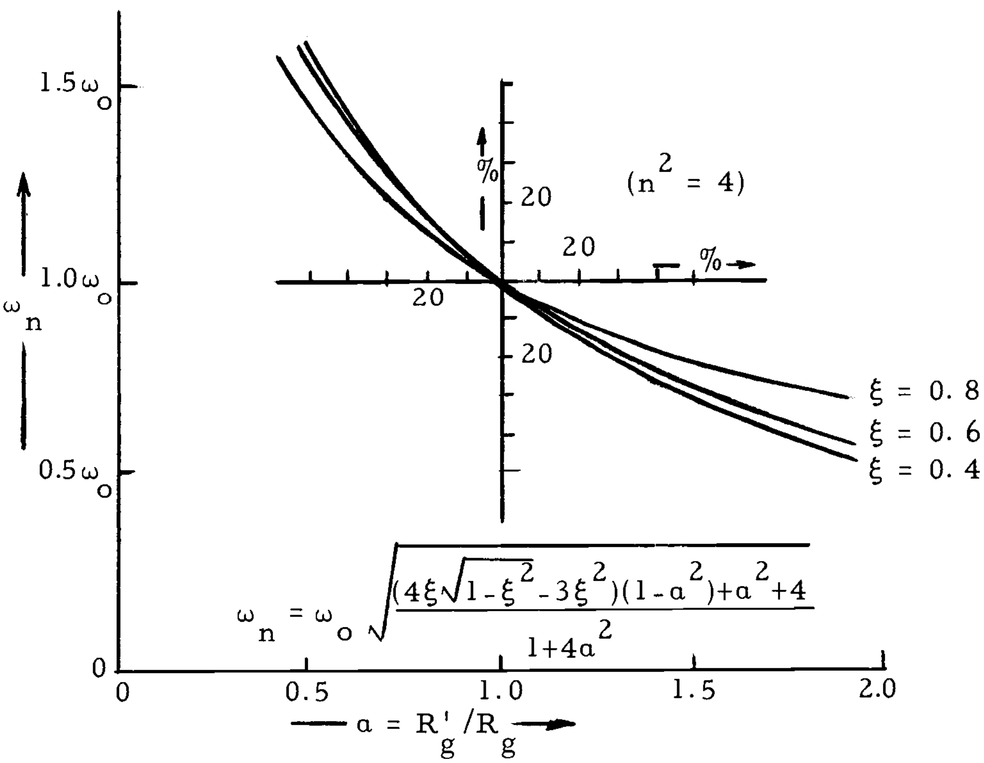

Figure 5-12. Resonant frequency vs a for single gyrator design method (A).

method. This can be seen by comparing Figures 5-5 and 5-6 to Figures 5-11 and 5-12. Using this method, the experimental results as indicated in Figure 5-14, which follows show quite good agreement with the theoretical case.

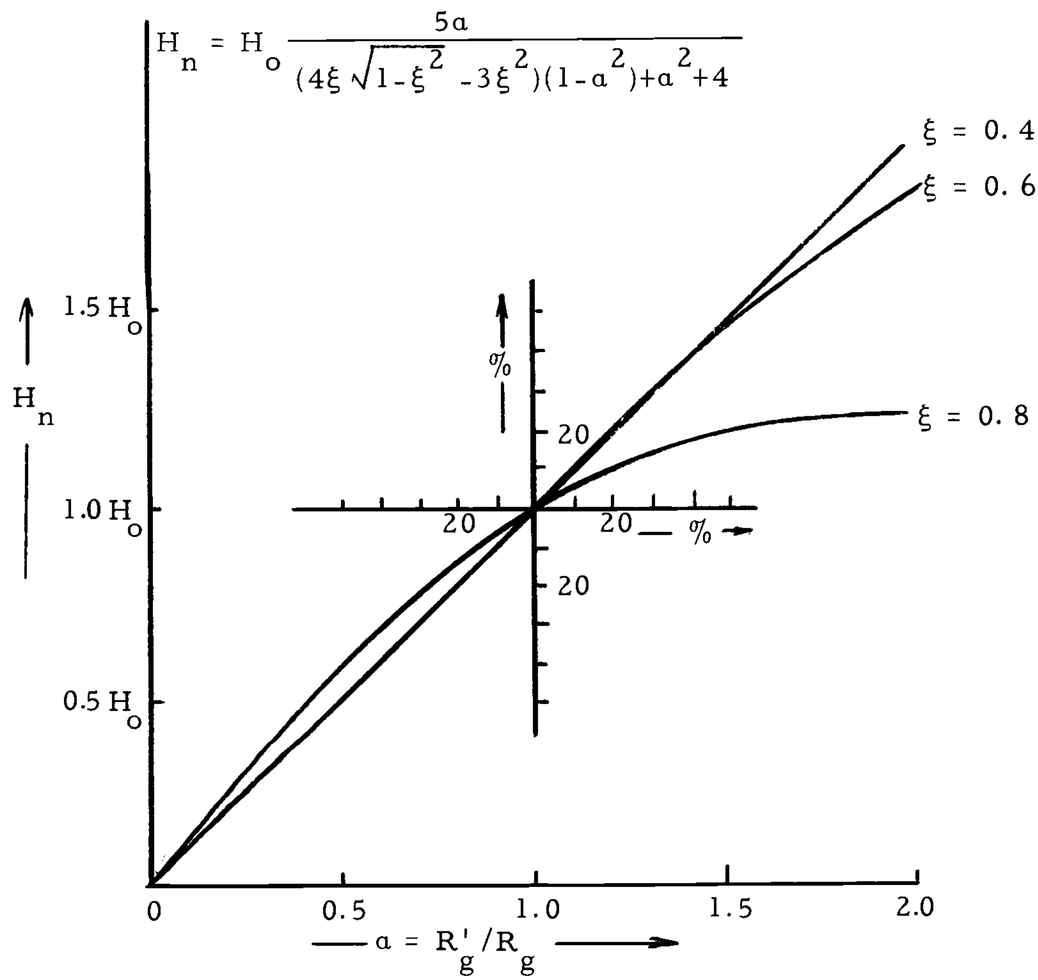

Figure 5-13. Gain vs a for single gyrator design method (A).

$$R_{a1} = \frac{(1+n^2)^2}{n^3} \frac{K_g^2}{k_o} \frac{\sqrt{1-\xi^2}}{\xi - \frac{1}{n}\sqrt{1-\xi^2}} = 625\ \Omega$$

$$R_{a2} = \frac{Hn^2}{n^2} \frac{R_g^2}{k_o} = 62.5\ \Omega$$

$$R_{b1} = \frac{k_o}{1+n^2} = 4000\ \Omega$$

$$R_{b2} = \frac{1}{n} k_o \frac{\sqrt{1-\xi^2}}{\xi - \frac{1}{n}\sqrt{1-\xi^2}} = 33.33\ \mathrm{K}\Omega$$

$$C_a = \frac{n^3}{(1+n^2)^2} \frac{k_o}{R_g^2 \omega_o} = 1.274\ \mu f$$

$$C_b = n \frac{1}{k_o \omega_o \sqrt{1-\xi^2}} = 0.0199\ \mu f$$

Select $n^2 = 4$, $\xi = 0.6$, $k_o = 2 \times 10^4$, $f = 1000$ c/s,

$\omega_o = 6280$ c/s, $R_g = 1000\ \Omega$

Gain $$H_o = \frac{1}{R_g} k_o \sqrt{1-\xi^2} \left(\xi - \frac{1}{n}\sqrt{1-\xi^2}\right) \frac{n}{n^2+1} = 1.28 = 2.144 \text{ db}$$

$$G_{12}(s) = \frac{H_o \omega_o^2}{s^2 + 2(0.6)\omega_o s + \omega_o^2}$$

Figure 5-14. The experimental result of RC-gyrator filter.

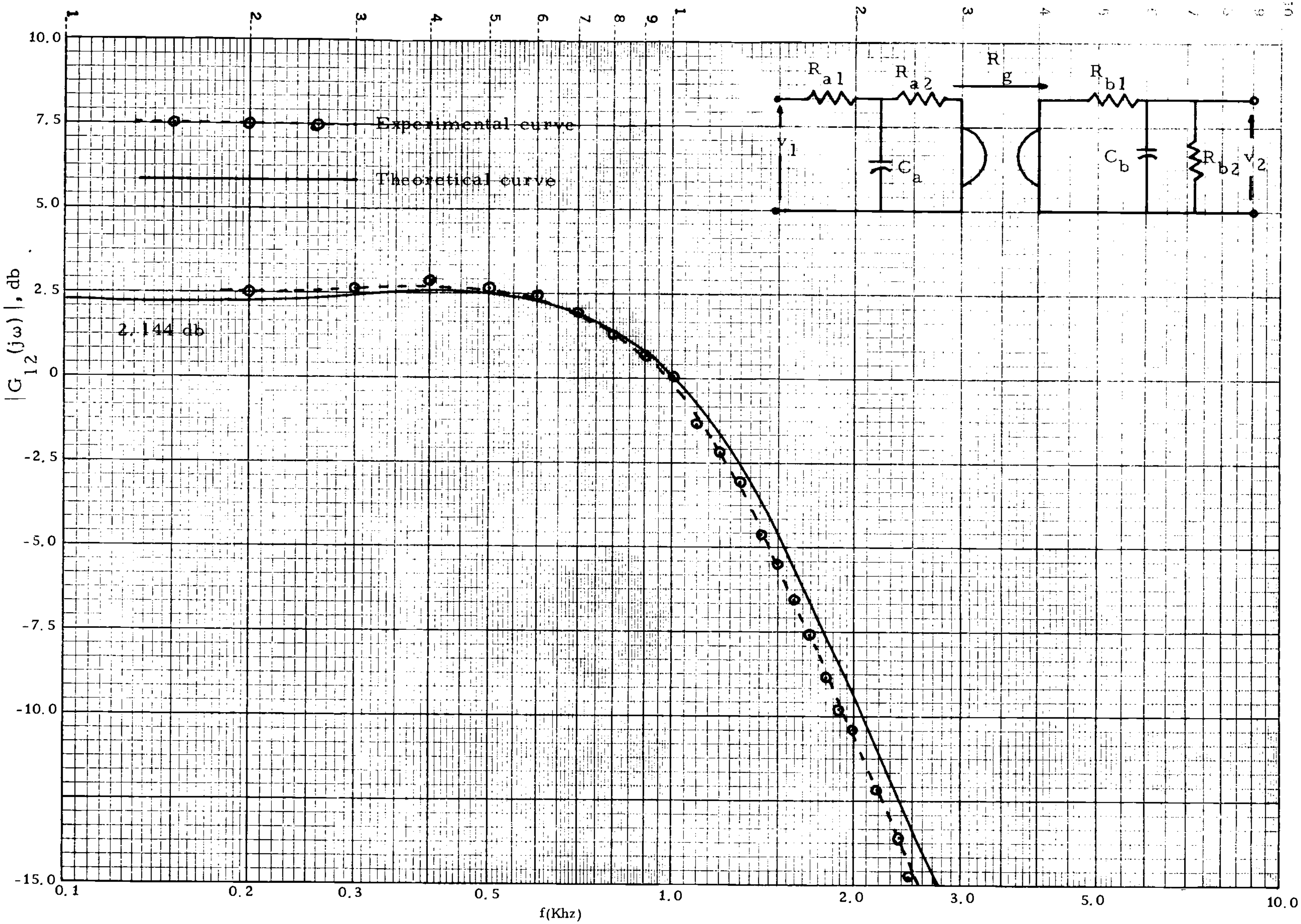

Figure 5-14. The experimental result of RC-gyrator filter.

(B). The optimum unique decomposition has the form

$$D(s) = \prod_{i=1}^{n/2} (s+a_i)^2 + B_{on} \prod_{i=1}^{(n/2)-1} (s+b_i)^2 . \tag{5-44}$$

Again, consider the low pass filter with damping ratio ξ and resonant frequency ω_o. It has the form

$$G_{12}(s) = \frac{H_o \omega_o^2}{s^2+2\xi\omega_o s+\omega_o^2} . \tag{5-45}$$

Recall Equation (5-15),

$$G_{12}(s) = \frac{N(s)/Q(s)}{D(s)/Q(s)} = - \frac{G y_{21} z_{21}}{y_{22}+G^2 z_{11}} . \tag{5-46}$$

Decompose the denominator into the form of

$$\frac{D(s)}{N(s)} = \frac{D_2(s)}{Q_2(s)} + G^2 \frac{D_1(s)}{Q_1(s)} = \frac{D_2(s)Q_1(s)+G^2 D_1(s)Q_2(s)}{Q_1(s)Q_2(s)} . \tag{5-47}$$

Therefore,

$$y_{22}(s) = \frac{D_2(s)}{Q_2(s)} , \qquad z_{11}(s) = \frac{D_1(s)}{Q_1(s)} . \tag{5-48}$$

where

$$Q(s) = Q_1(s)Q_2(s), \tag{5-49a}$$

$$D(s) = D_2(s)Q_1(s) + G^2 D_1(s)Q_2(s). \tag{5-49b}$$

The optimum form of $D(s)$ can be found in the example on page 18:

$$D(s) = s^2 + 2\xi\omega_o s + \omega_o^2 = (s+\xi\omega_o)^2 + \omega_o^2(1-\xi^2). \tag{5-50}$$

Thus

$$D_2(s)Q_1(s) = (s+\xi\omega_o)^2, \tag{5-51a}$$

$$D_1(s)Q_2(s) = 1, \tag{5-51b}$$

and

$$G = \omega_o\sqrt{1-\xi^2}\,. \tag{5-51c}$$

Assign

$$D_2(s) = s + \xi\omega_o, \tag{5-52a}$$

$$Q_1(s) = s + \xi\omega_o, \tag{5-52b}$$

$$D_1(s) = 1, \tag{5-52c}$$

and

$$Q_2(s) = 1. \tag{5-52d}$$

Then

$$y_{22} = s + \xi\omega_o, \tag{5-53a}$$

and

$$z_{11} = \frac{1}{s+\xi\omega_o}\,. \tag{5-53b}$$

are found from the numerator

$$\frac{N(s)}{Q(s)} = -Gy_{21}z_{21} = \frac{H_o\omega_o^2}{s+\xi\omega_o}\,. \tag{5-54}$$

Thus

$$-y_{21} = H_1 \tag{5-55a}$$

$$z_{21} = \frac{H_2}{s+\xi\omega_o}\,, \quad \text{and} \quad H_1H_2 = H_o\omega_o^2. \tag{5-55b}$$

The RC network to the left of the gyrator can be obtained by y_{22} and $-y_{21}$. Similarly, the network to the right of the gyrator can be found by z_{11} and z_{12}. The complete network is shown in Figure 5-15.

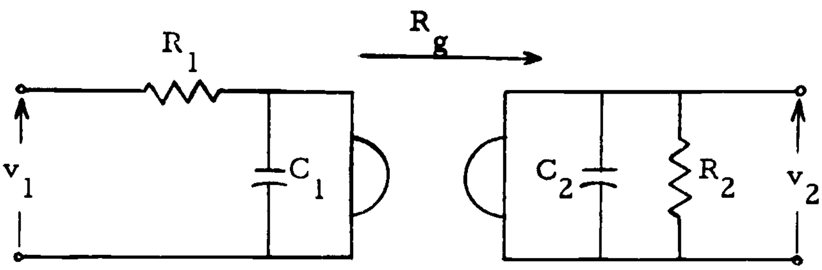

Figure 5-15. The realization of Equation (5-45).

where

$$R_1 = \frac{1}{\xi\omega_o}, \quad R_2 = \frac{1}{\xi\omega_o}, \quad C_1 = 1, \quad C_2 = 1,$$

and

$$G = \omega_o\sqrt{1-\xi^2}$$

The transfer function of Figure 5-15 in terms of R_1, R_2, C_1, C_2 and G, can be written as

$$G_{12}(s) = \frac{\frac{G}{R_1C_1C_2}}{s^2+s\left(\frac{1}{R_1C_1}+\frac{1}{R_2C_2}\right)+\frac{G^2+\frac{1}{R_1R_2}}{C_1C_2}}$$

$$= \frac{G\xi\omega_o}{s^2+2\xi\omega_o s+\omega_o^2} \tag{5-56}$$

The gyration resistance and the gyration conductance are changed from R_g to R_g' and G to G', respectively.

Let

$$a = \frac{R_g'}{R_g} = \frac{G}{G'} \ . \tag{5-57}$$

Then the transfer function $G_{12}(s)$ is changed to

$$\begin{aligned} G_{12}(s) &= \frac{\frac{G}{a}\xi\omega_o}{s^2+2\xi\omega_o s+(\frac{G}{a})^2+\xi^2\omega_o^2} \\ &= \frac{H_n\omega_n^2}{s^2+2\xi_n\omega_n s+\omega_n^2} \ . \end{aligned} \tag{5-58}$$

Thus, when the gyration resistance or the gyration conductance is changed, the damping ratio ξ, resonant frequency ω_o and gain H_o are changed to

$$\omega_n = \sqrt{(\frac{G}{a})^2+\xi^2\omega_o^2} = \frac{\omega_o}{a}\sqrt{1+\xi^2(a^2-1)}, \tag{5-59a}$$

$$\xi_n = \frac{\xi\omega_o}{\omega_n} = \frac{a\xi}{\sqrt{1+\xi^2(a^2-1)}} \ , \tag{5-59b}$$

and

$$H_n = \frac{a}{(1-\xi^2)+a^2\xi^2} H_o \ , \tag{5-59c}$$

respectively.

Figure 5-16 shows the percent change in damping ratio ξ_n, with percent change in R_g. Figure 5-16 shows the percent change in

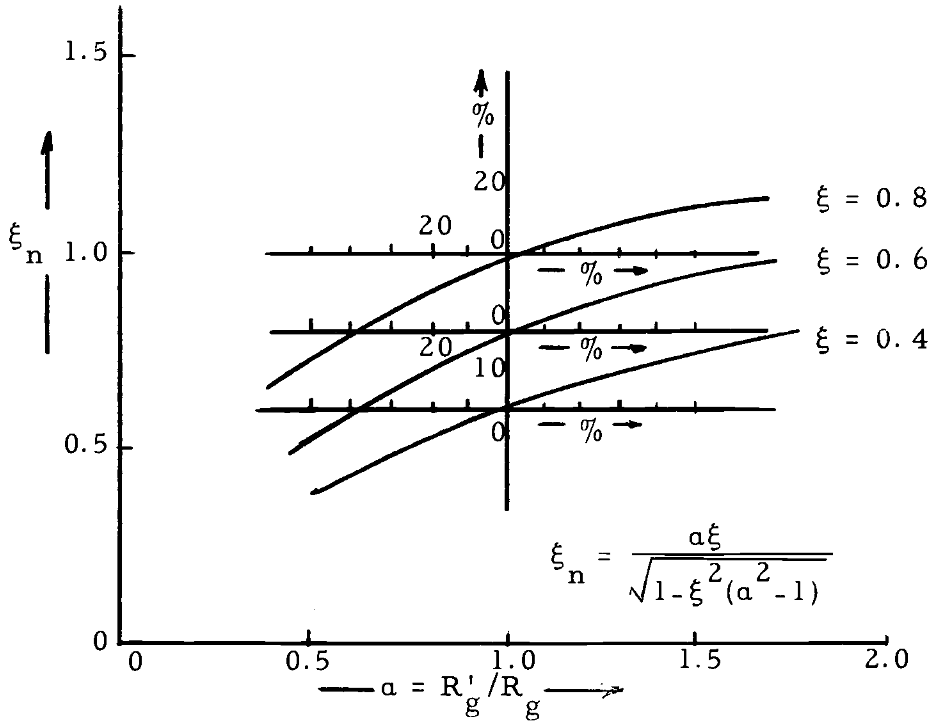

Figure 5-16. Damping ratio vs a for single gyrator design method (B).

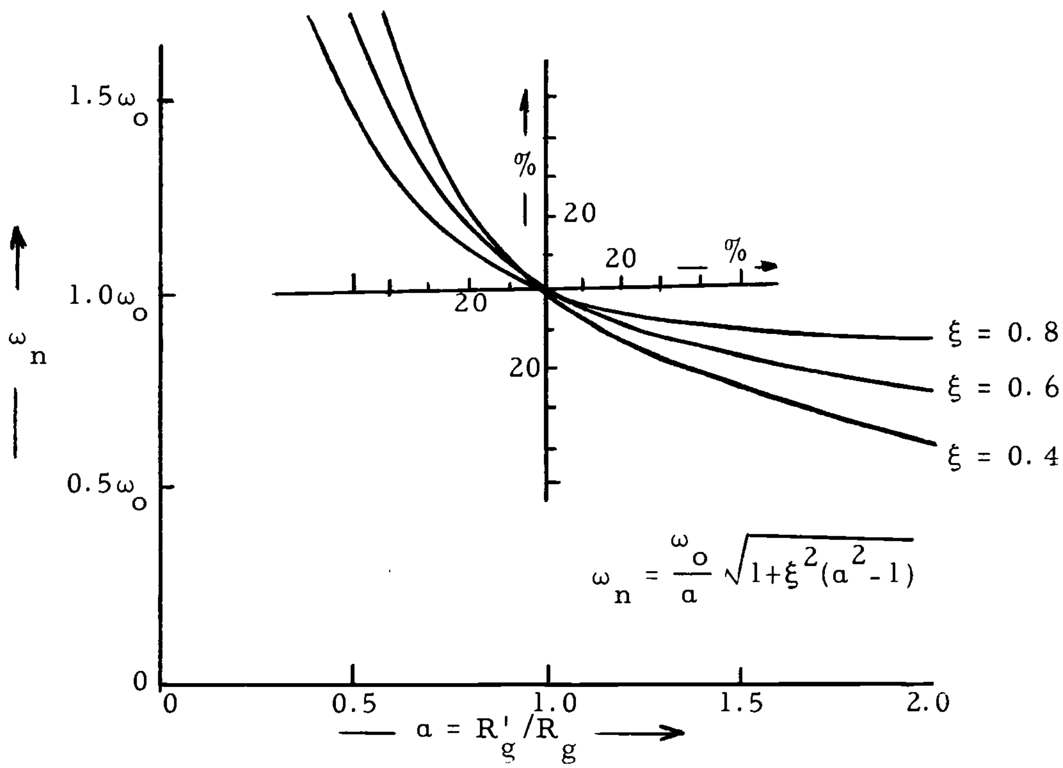

Figure 5-17. Resonant frequency vs a for single gyrator design method (B).

resonant frequency ω_n, with percent change in R_g. Figure 5-18 shows the percent change in dc gain, H_n, with respect change in R_g. Compare Figure 5-16 and 5-15 to Figure 5-11 and 5-12 and Figure 5-5 and 5-6. This comparison shows that the single gyrator design method always has lower sensitivity than the direct design method.

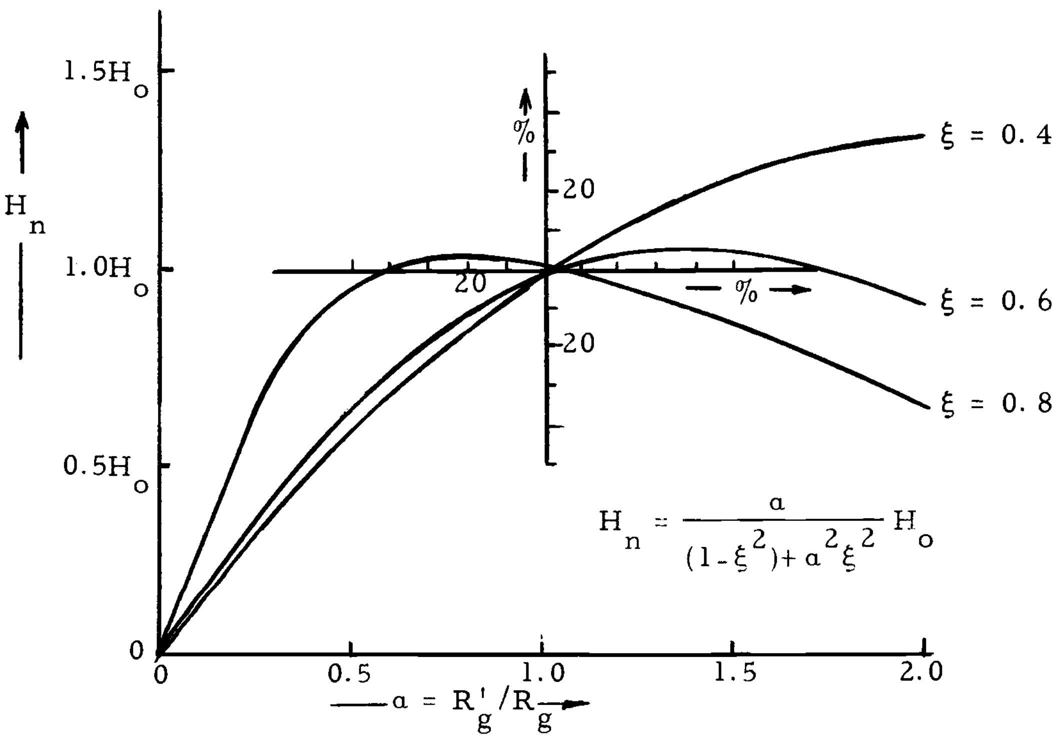

Figure 5-18. Gain vs R_g for single gyrator design method (B).

VI. SUMMARY

Two methods of active filter synthesis were derived. The first was replacing inductors in the conventional LC filter with gyrators and capacitors. The second was using a single gyrator cascaded by two RC two port networks. The gyrator is realized by cascading an ideal negative impedance inverter (NIV) and a negative impedance converter (NIC). Each NIV and NIC is realized by using a single operational amplifier. Therefore, the gyrator can be realized by using two operational amplifiers. It is to be noted that the gyration resistance can easily be adjusted by adjusting the passive elements of the NIV.

In RC-gyrator synthesis, although the realization of the gyrator is much more complicated than that of the NIC or of controlled sources, it has the disadvantage of not being able to provide large amounts of gain. However, it does have the following advantages. First, from its lossless nature, the gyrator can never be unstable. Second, since a capacitor in general has a higher quality factor than an inductor, gyration using a capacitor produces a better inductor than that now available. Third, it provides lower sensitivity than comparable realization using controlled sources or NICs. These advantages make the gyrator realization very attractive.

The applications of integrated circuit technology in active RC network synthesis have received much attention recently, especially in microminiaturization. In active RC integration network design, the designer may no longer select passive elements and interconnect them to achieve a network, but rather must make the passive components simultaneously with the active elements in the integration procedure. In integrated circuit technology the initial tolerances of the resistors and capacitors are still within certain limits. Therefore, the sensitivity minimization problem is not a single parameter sensitivity problem but a multiparameter sensitivity problem The sensitivity minimization of the polynomial decomposition applied in this thesis is due only to the change in active elements. In this thesis, only the single-parameter sensitivity was considered. Multiparameter sensitivity of integratable active RC networks is suggested as a topic of future study.

BIBLIOGRAPHY

1. Antoniou, A. Gyrator using operational amplifiers. Electron Letters 3:350-352. 1967.

2. Burr-Brown Research Corporation. Handbook of operational amplifier active RC networks. 2d ed. Tucson, 1965. 104 p.

3. Bogert, B. P. Some gyrator and impedance inverter circuits. Proceedings of the Institute of Radio Engineering 43:793-796. 1955.

4. Calahan, D. A. Notes on the Horowitz optimization procedure. IRE transactions on circuit theory. CT7:252-254. 1960.

5. ______________ Restrictions of the natural frequencies of an RC-RL network. Journal of the Franklin Institute 272:112-133. 1961.

6. ______________ Sensitivity minimization in active RC synthesis. IRE transactions on circuit theory CT9:38-42. 1962.

7. Horowitz, I. M. Optimization of negative impedance conversion methods of active RC synthesis. IRE transactions on circuit theory CT6:296-303. 1959.

8. Huelsman, L. P. Circuits, matrices and linear vector spaces. New York, McGraw-Hill, 1963. 281 p.

9. ______________ Theory and design of active RC circuits. New York, McGraw-Hill, 1968. 297 p.

10. Lundry, W. Ralph. Negative impedance circuits--some basic relation and limitations. IRE transactions on circuit theory CT4:132-139. 1957.

11. Mitra, Sanjit, K. Synthesing active filters. IEEE Spectrum. 6-1:47-63. 1969.

12. Morse, A. Stephen. The use of operational amplifiers in active network theory. Proceedings of National Electronics Conference 29:748-752. 1964.

13. Shenoi, B. A. Practical realization of gyrator circuit and RC gyrator filters. IEEE transactions on circuit theory 12:374-380. 1965.

14. Su, K. L. Active network synthesis. New York, McGraw-Hill, 1965. 369 p.

15. Tellegen, B. D. H. The gyrator, A new network element. Philips Research Reports 3:81-101. 1948.

16. Van Valkenburg, M. E. Introduction to modern network synthesis. New York, Wiley, 1960. 498 p.